Supporting Information

Recombinant Silicateins as a Model Biocatalyst in Organosiloxane Chemistry

S. Yasin Tabatabaei Dakhili,[a,b] Stephanie A. Caslin,[a,b] Abayomi S. Faponle,[a,c] Peter Quayle,[b] Sam P. de Visser,[a,c] Lu Shin Wong [a,b] *

[a] Manchester Institute of Biotechnology, University of Manchester, 131 Princess Street, Manchester M1 7DN, UK.

[b] School of Chemistry, University of Manchester, Oxford Road, Manchester M13 9PL, UK.

[c] School of Chemical Engineering and Analytical Science, University of Manchester, Oxford Road, Manchester M13 9PL, UK.

Email: l.s.wong@manchester.ac.uk

Contents

1 Supplementary Results.

1.1 Purification of silicateins

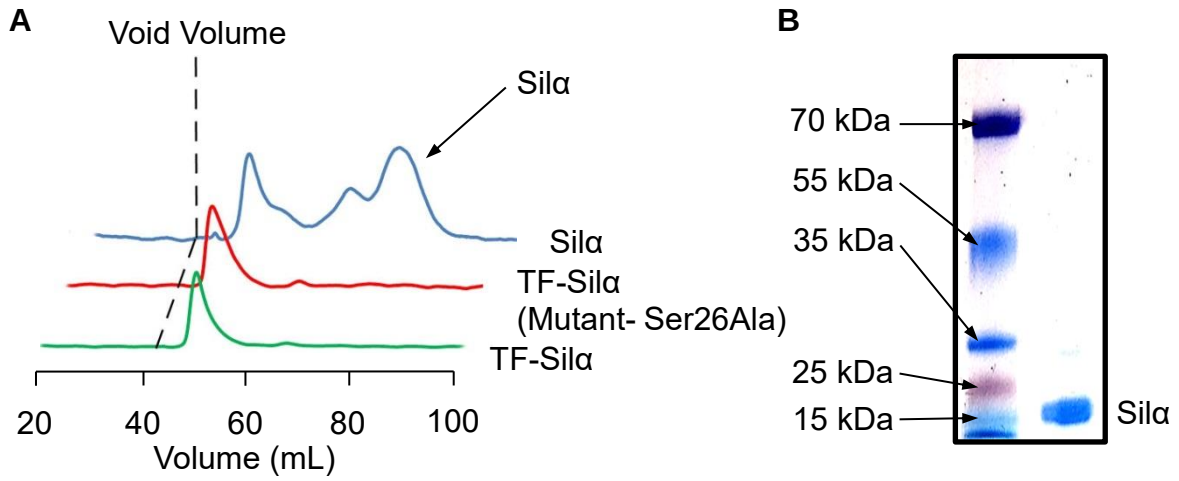

Figure S1. (A) SEC chromatograms for TF-Silα and TF-Silα(Ser26Ala) after purification and concentration, and for Silα during the final purification step; and (B) image of non-denaturing PAGE gel for Silα (right lane) with reference marker proteins (left lane).

1.2 Circular dichroism (CD) spectroscopy

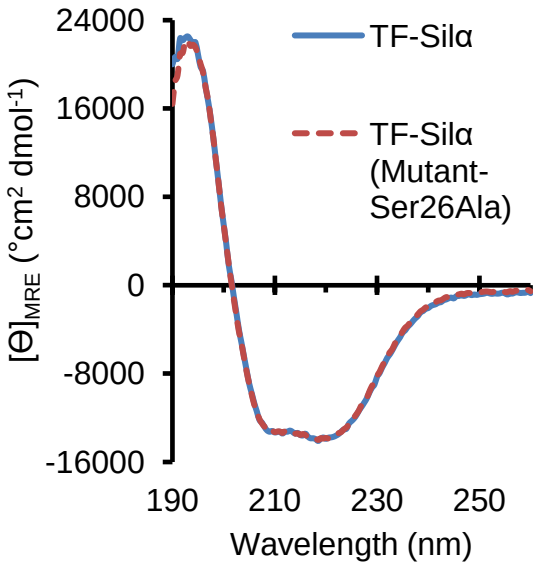

Figure S2. CD Spectra plots of mean residue ellipicity against wavelength for TF-Silα and TF-Silα(Ser26Ala).

Table S1. Estimated proportions of secondary structure in TF-Silα calculated by the CDNN algorithm using the CD spectrum in Figure 2.

Wavelength (nm)	**190-260**	**195-260**	**200-260**	**205-260**	**210-260**	**Average**
α-Helix	31.70%	31.25%	31.15%	32.11%	31.22%	**31.49%**
Antiparallel	9.97%	10.12%	9.03%	8.05%	8.62%	**9.16%**
Parallel	8.67%	8.93%	9.23%	9.24%	9.02%	**9.02%**
β-Turn	17.15%	16.96%	17.06%	16.70%	17.05%	**16.98%**
Rndm. Coil	32.50%	32.74%	33.53%	33.90%	34.09%	**33.35%**
Total Sum	100.00%	100.00%	100.00%	100.00%	100.00%	**100.00%**

Table S2. Estimated proportions of secondary structure in TF-Silα(Ser26Ala) calculated by the CDNN algorithm using the CD spectrum in Figure 2.

Wavelength (nm)	**190-260**	**195-260**	**200-260**	**205-260**	**210-260**	**Average**
α-Helix	31.31%	31.25%	31.15%	32.11%	31.22%	**31.41%**
Antiparallel	10.34%	10.12%	9.03%	8.05%	8.62%	**9.23%**
Parallel	8.75%	8.93%	9.23%	9.24%	9.02%	**9.03%**
β-Turn	17.20%	16.96%	17.06%	16.70%	17.05%	**16.99%**
Rndm. Coil	32.41%	32.74%	33.53%	33.90%	34.90%	**33.33%**
Total Sum	100.00%	100.00%	100.00%	100.00%	100.00%	**100.00%**

Table S3. Comparison of proportions of secondary structure in TF-Silα and TF-Silα(Ser26Ala).

	TF-Silα (approximated from crystallographic structures)[a]	TF-Silα (from Table S1)	TF-Silα(Ser26Ala) (from Table S2)
α-Helix	33.18%	31.49%	31.41%
Antiparallel	9.29%	9.16%	9.23%
Parallel	5.22%	9.02%	9.03%
β-Turn	16.36%	16.98%	16.99%
Rndm. Coil	32.95%	33.35%	33.33%
Total Sum	100.00%	100.00%	100.00%

[a] See Section 2.3 below for details of calculations.

1.3 Silicomolybdic acid assay.

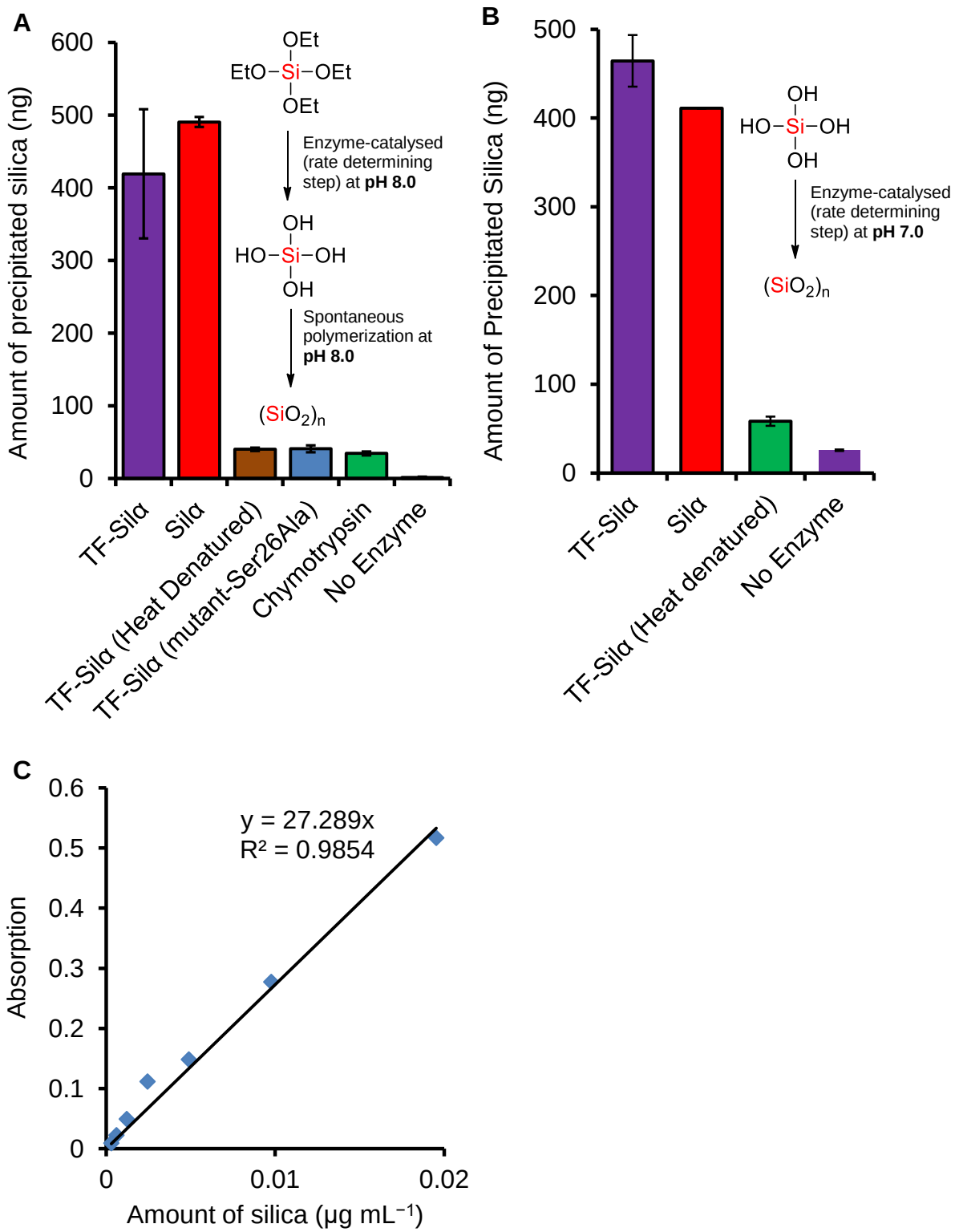

Figure S3. Graphs of the amount of silica produced after 1 h, as quantified by the silicomolybdic acid assay from the (A) hydrolysis of TEOS and (B) condensation of pre-hydrolyzed TEOS. (C) Graph from the UV-Vis calibration of the silicomolybdic assay.

1.4 Colorimetric silyl ether screening assays.

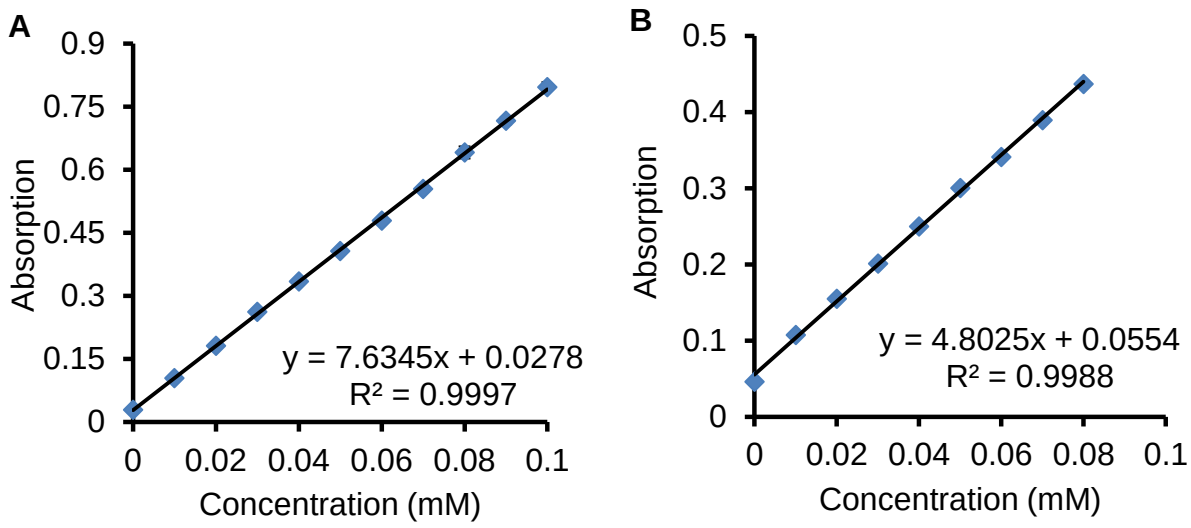

Figure S4. Calibration graphs of UV-Vis absorption at 405 nm against concentration of 4-nitrophenol (A) or 4-nitroaniline (B) in buffed solutions (5% v/v dioxane, 50 mM Tris, 100 mM NaCl, pH 8.5).

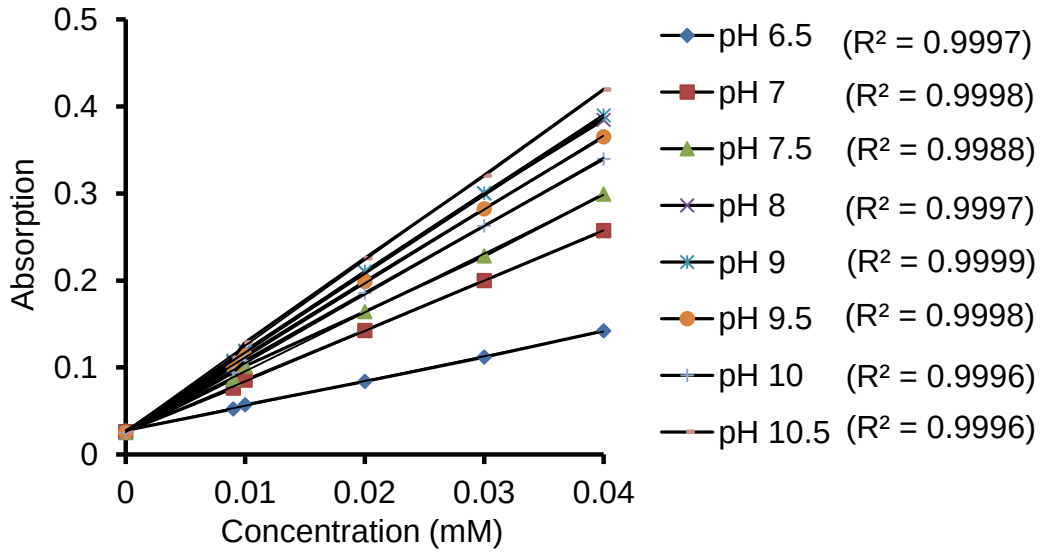

Figure S5. Calibration graph of UV-Vis absorption at 405 nm against the concentration of 4-nitropheno1 from pH 6.5 to 10.5 in the buffer solution (5% v/v dioxane, 50 mM Tris, 100 mM NaCl).

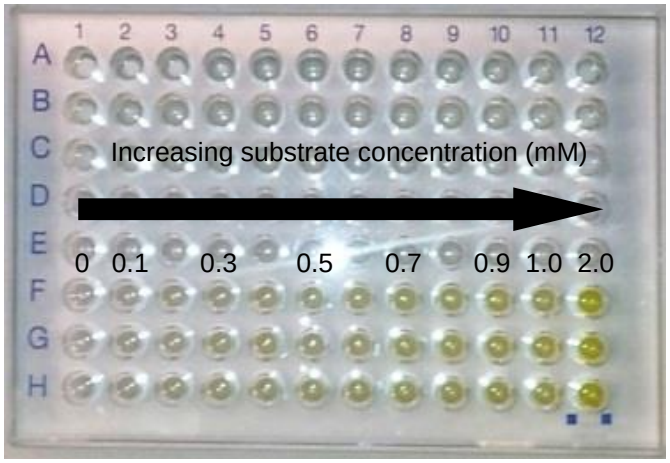

Figure S6. Photograph of 96-well microtitre plate showing example assays where a visually observable color was generated upon hydrolysis of **1**.

1.5 Substrate hydrolysis time course experiments and Michaelis-Menten kinetics calculations.

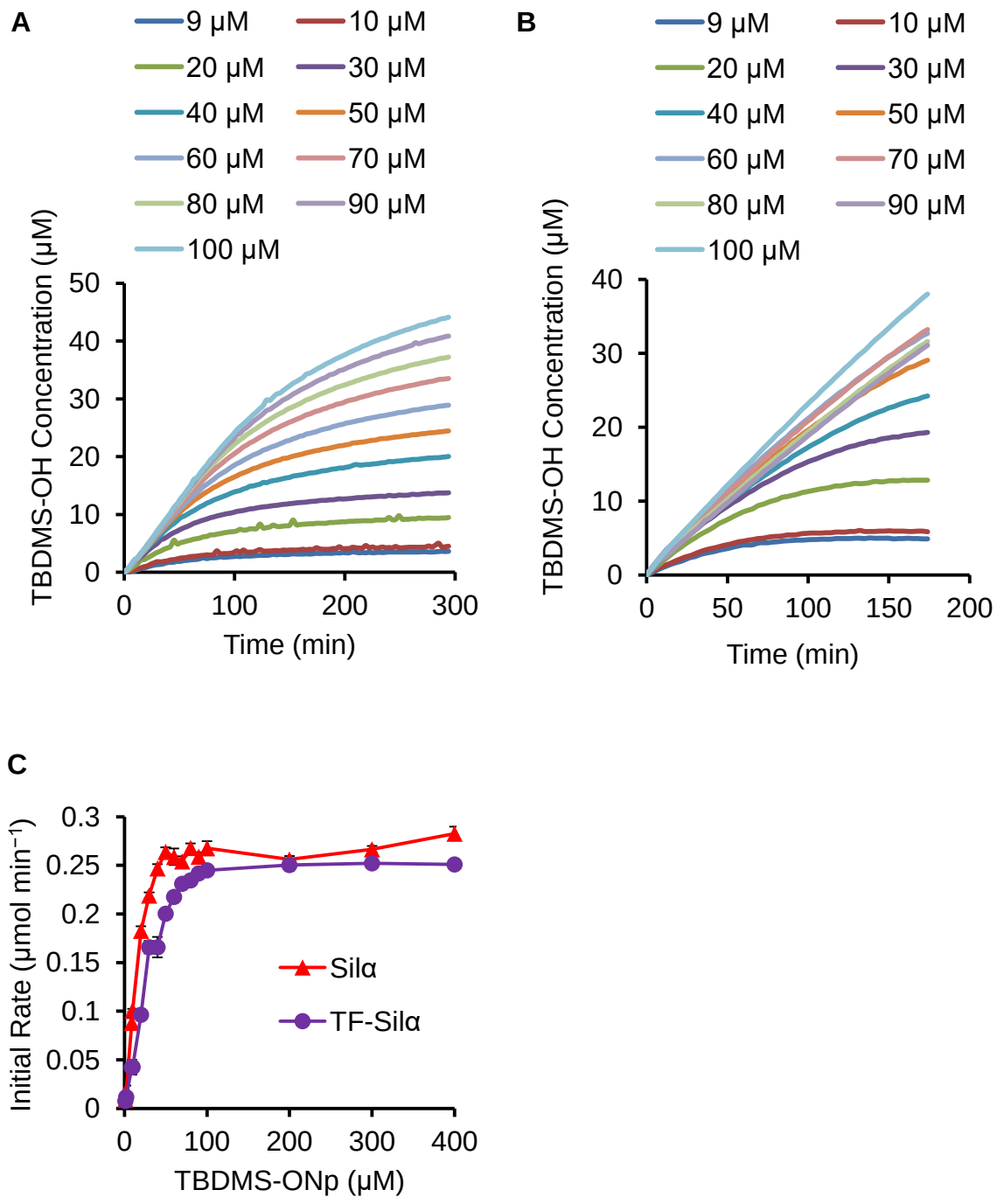

Figure S7. Graph of the concentration of 4-nitrophenol against time for the hydrolysis catalyzed by TF-Silα and Silα for **1** (A and B, respectively) and the associated Michaelis–Menten saturation curves (C).

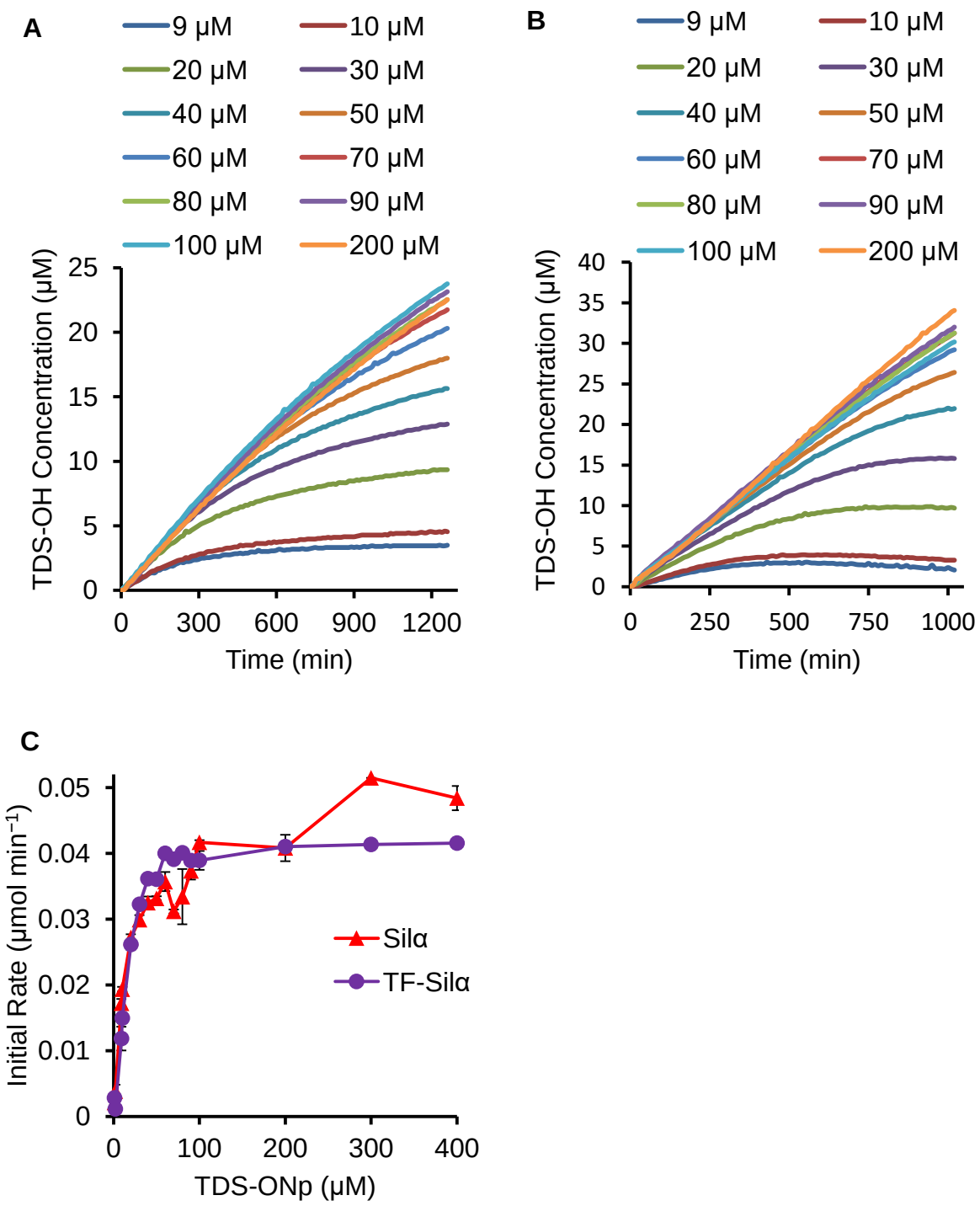

Figure S8. Graph of the concentration of 4-nitrophenol against time for the hydrolysis catalyzed by TF-Silα and Silα for **2** (A and B, respectively) and the associated Michaelis–Menten saturation curves (C).

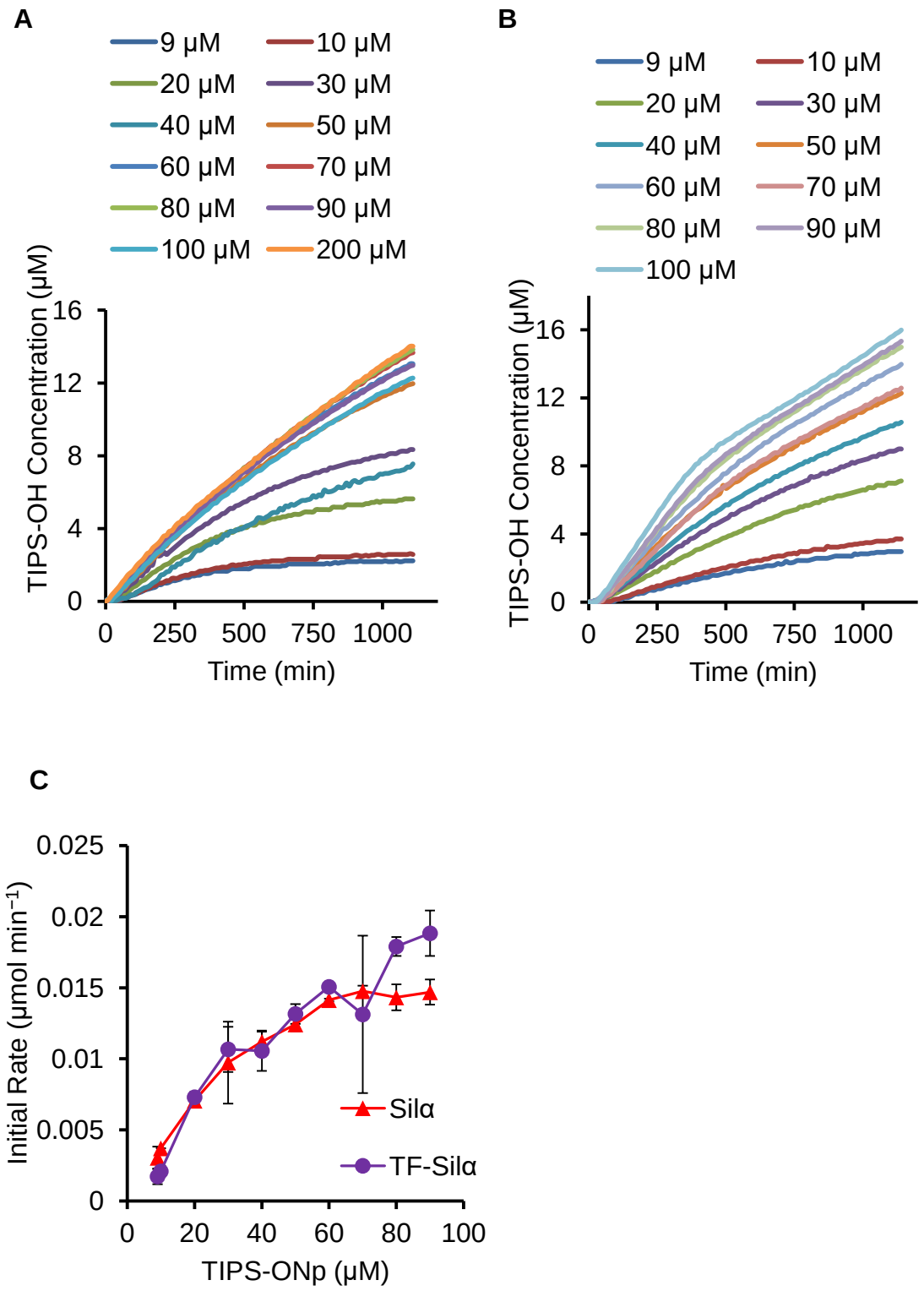

Figure S9. Graph of the concentration of 4-nitrophenol against time for the hydrolysis catalyzed by TF-Silα and Silα for **3** (A and B, respectively) and the associated Michaelis–Menten saturation curves (C).

1.6 Molecular Dynamics Simulations

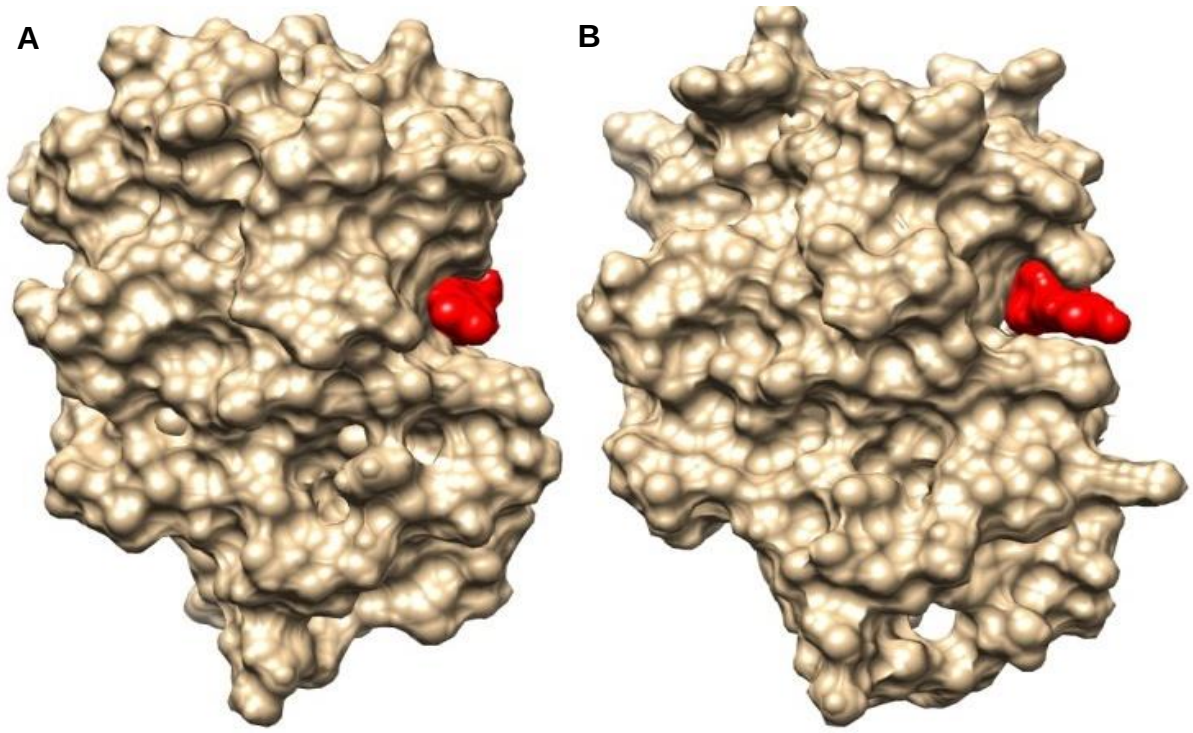

Figure S10. Images showing the location of substrate **1** (red) with respect to the protein during the non-constrained MD simulation at: (A) the starting point (0 ns) and; (B) the end of the simulation (1 ns).

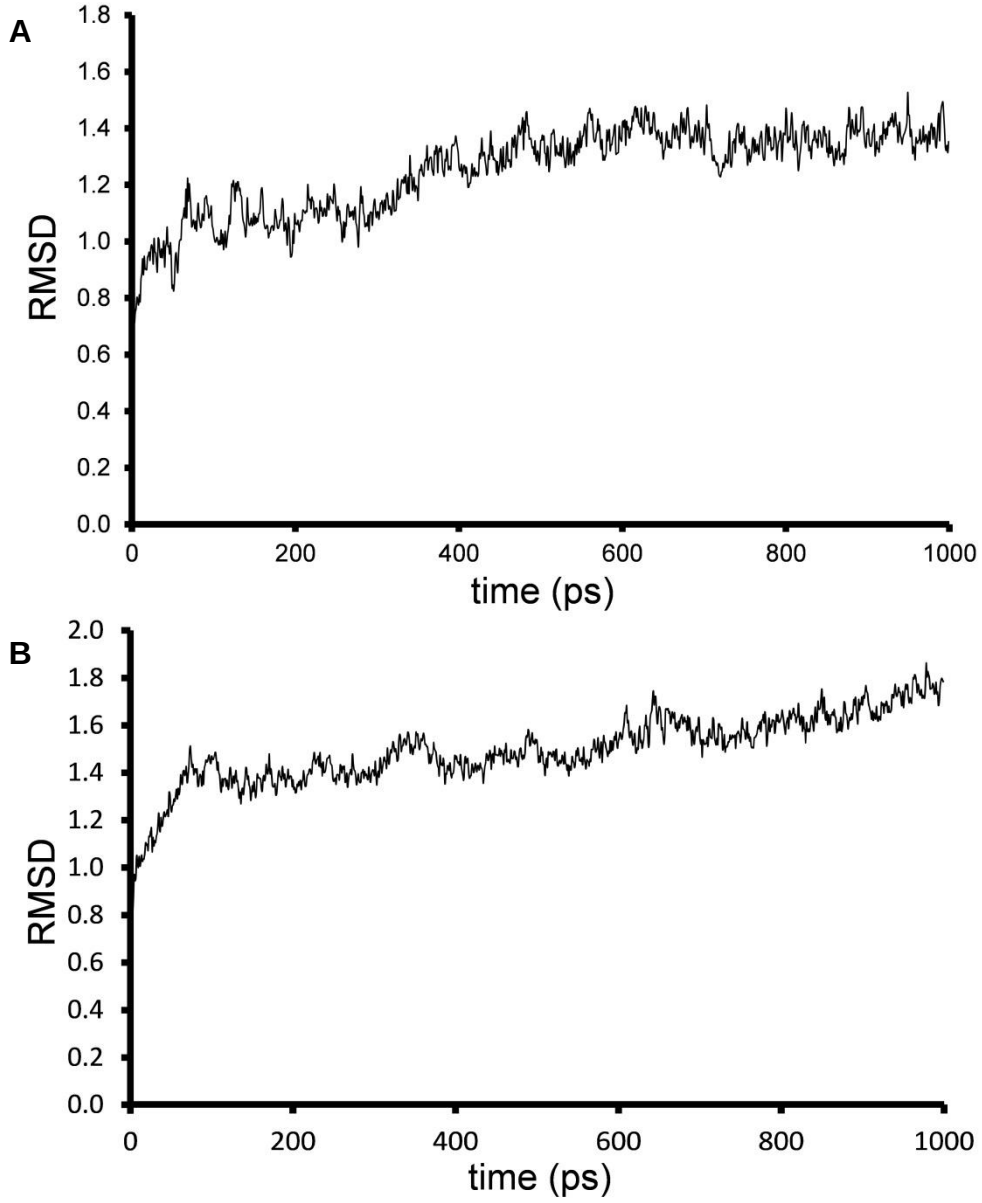

Figure S11. Graph of root mean squared interatomic distances (RMSD) against time for the simulated models using (A) the unconstrained substrate and (B) geometry constrained substrate.

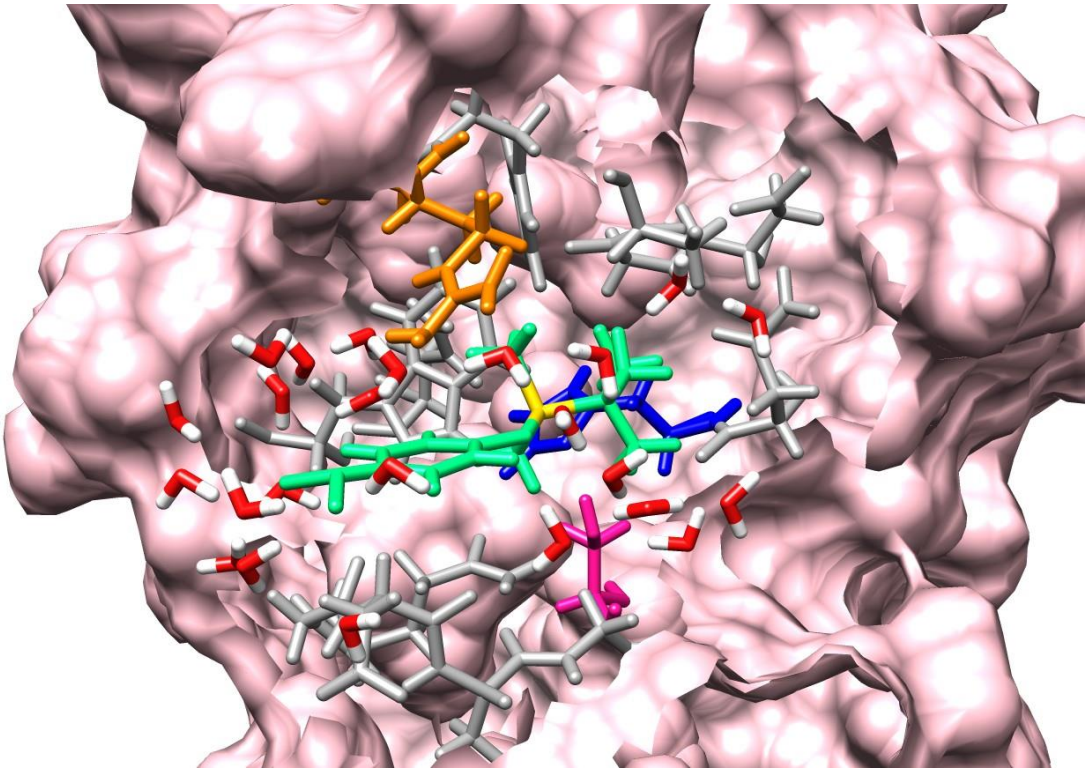

Figure S12. Image of **1** bound to Silα at the end of the MD simulation with the water molecules within 4 Å of the substrate now shown (in red and white). This image is shown with the same perspective and color coding as Figure 6 in all other respects.

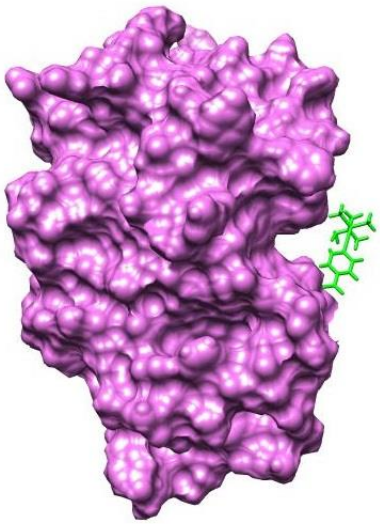

Figure S13. Image of the overall protein structure at the end of the MD simulation with **1** in a constrained geometry, showing the unbound substrate.

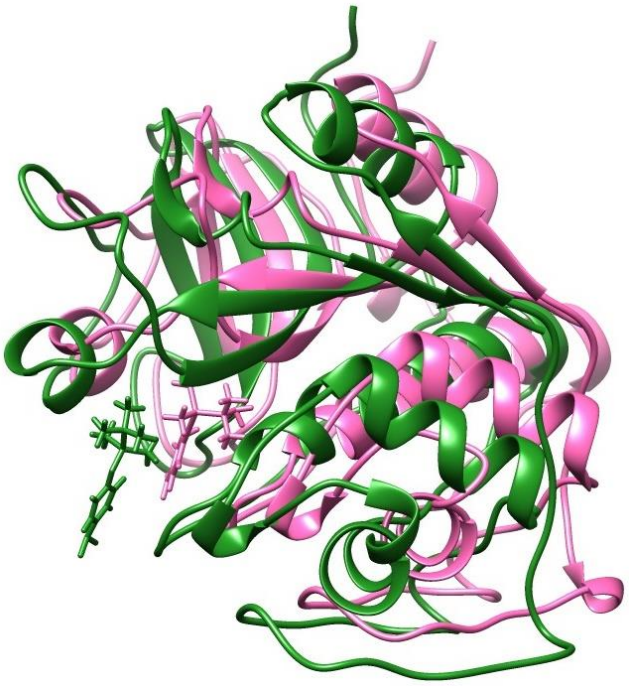

Figure S14. Overlay of the starting (in pink) and final (in green) structures of the 1ns MD simulation of non-constraint protein and substrate.

1.7 Condensation reactions in organic solvents.

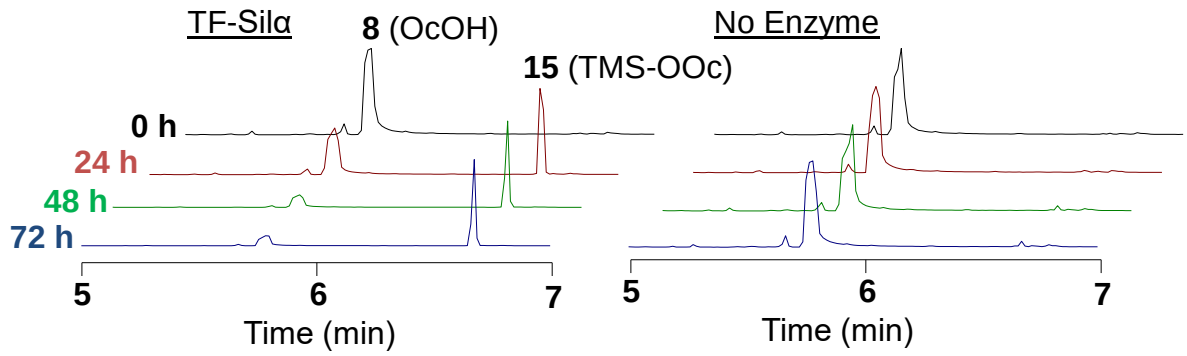

Figure S15. The GC chromatograms for the condensation of **15** from **8** and **9**.

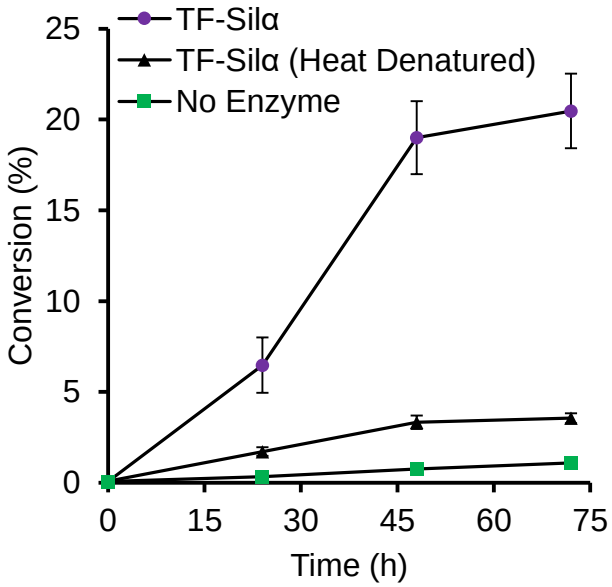

Figure S16. Graph of percentage conversion to the silyl ether **15** against reaction time, as determined by GC-MS analysis of the reaction products (calibrated using data from Figure S17). Assays are conducted with 5 mol. eq. of silanol relative to octanol at 22 °C.

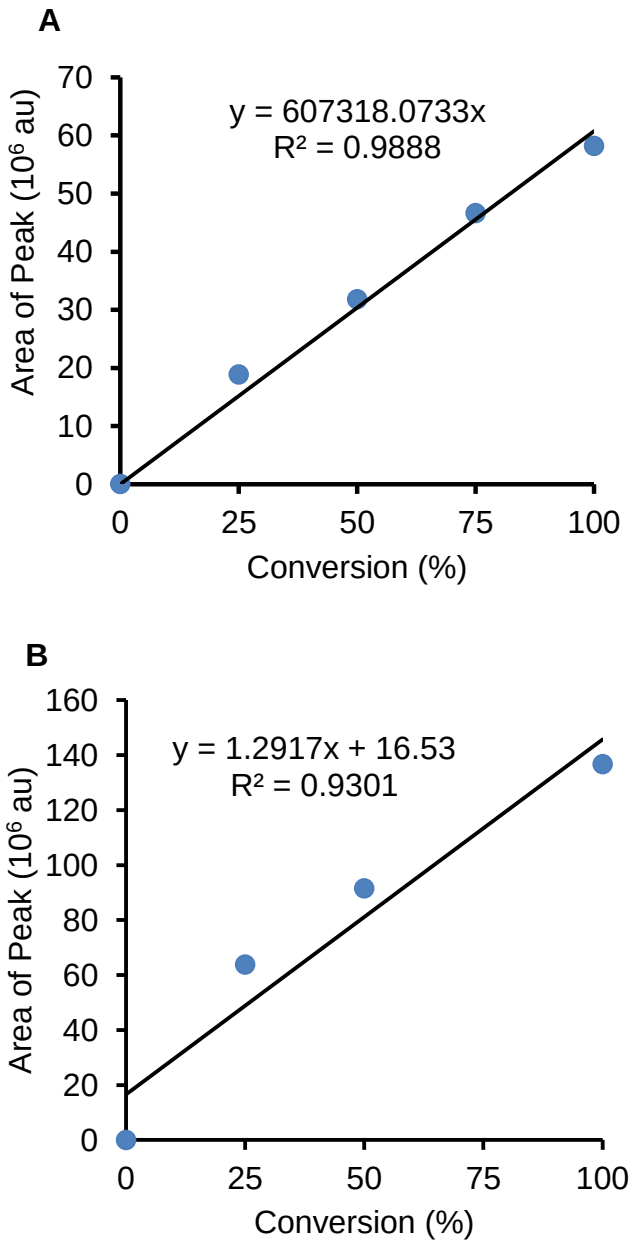

Figure S17. (A) Calibration graph of area under the peak corresponding to silyl ether **15** in the GC-MS trace against percentage conversion based on equivalent amounts of synthetic standards. (B) Calibration graph of area under the peak corresponding to silyl ether **28** in the GC-MS trace against percentage conversion.

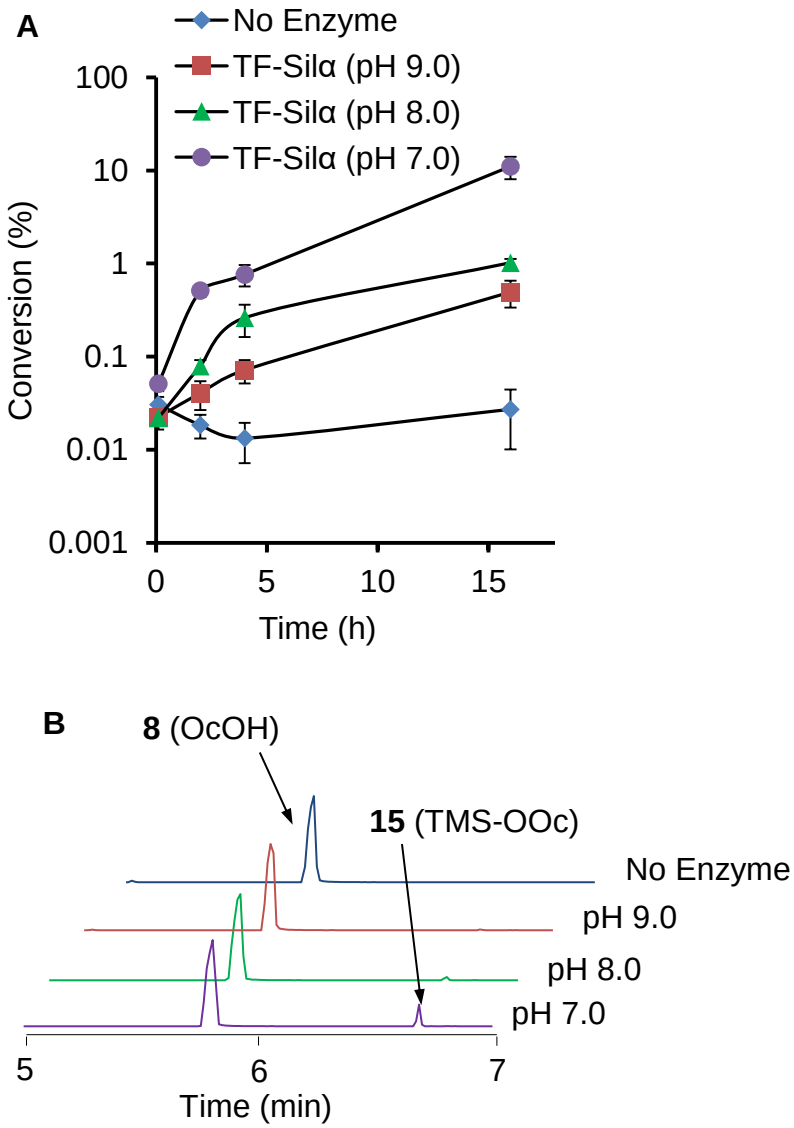

Figure S18. (A) Graph of percentage conversion of **8** to **15** against reaction time at three different pH values (9, 8 and 7), as determined by GC-MS analysis of the reaction products. (B) GC chromatograms of the condensation reactions after 16 h.

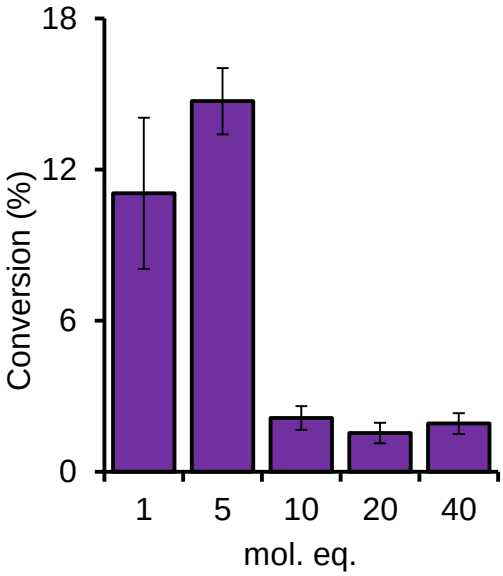

Figure S19. Graph of percentage conversion of octanol **8** to **15** against number of molar equivalents of silanol **9** used relative to the alcohol after 24 h at 22 °C, as determined by GC-MS analysis of the reaction products.

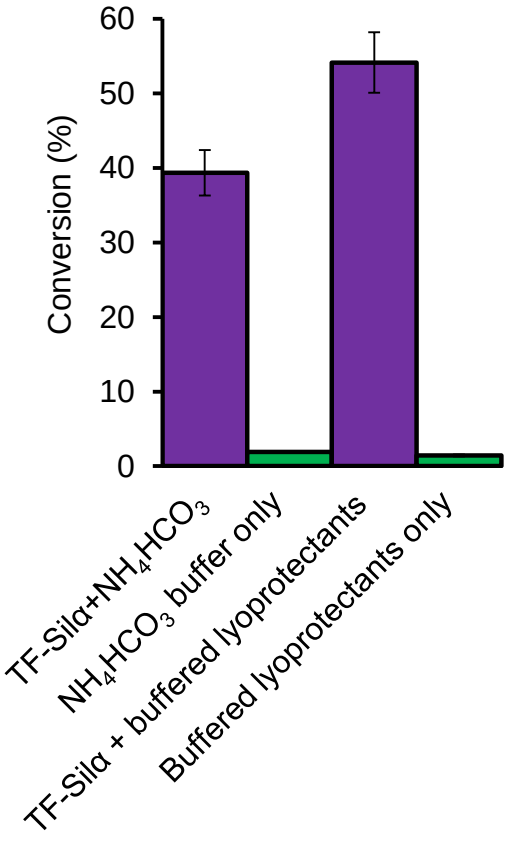

Figure S20. Graph of percentage conversion of **8** to **15** comparing enzyme preparations containing lyoprotectants, buffered with potassium phosphate to pH 7, after 24 h at 75 °C.

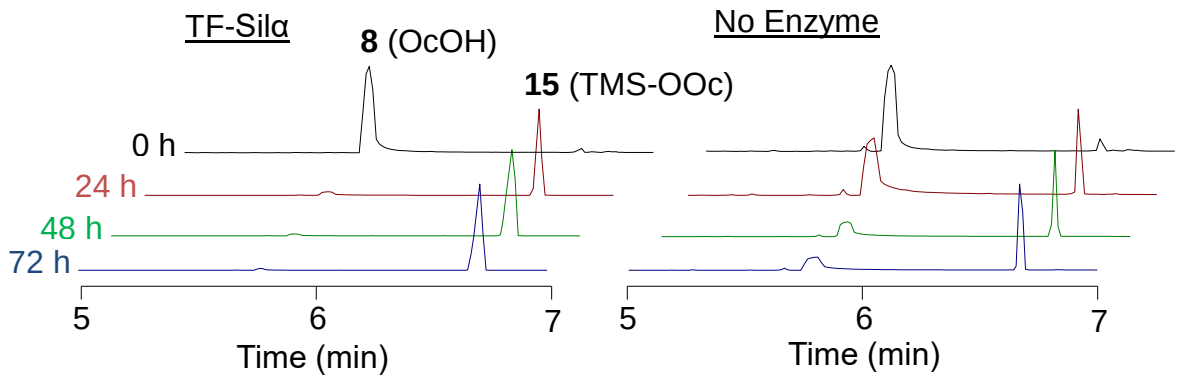

Figure S21. The GC chromatograms for the condensation of **15** from **8** and **9** using optimized conditions (75 °C , lyoprotectants added)**.**

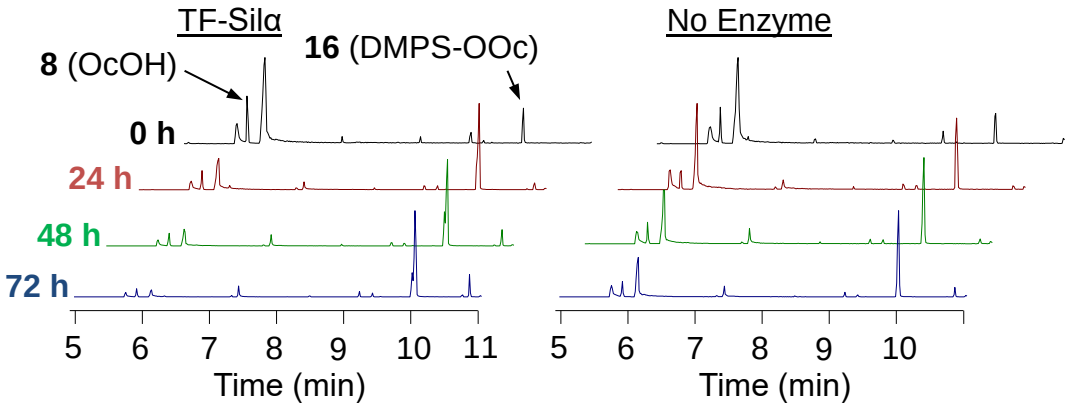

Figure S22. The GC chromatograms for the condensation of **16** from **8** and **10** using optimized conditions (75 °C, lyoprotectants added)**.**

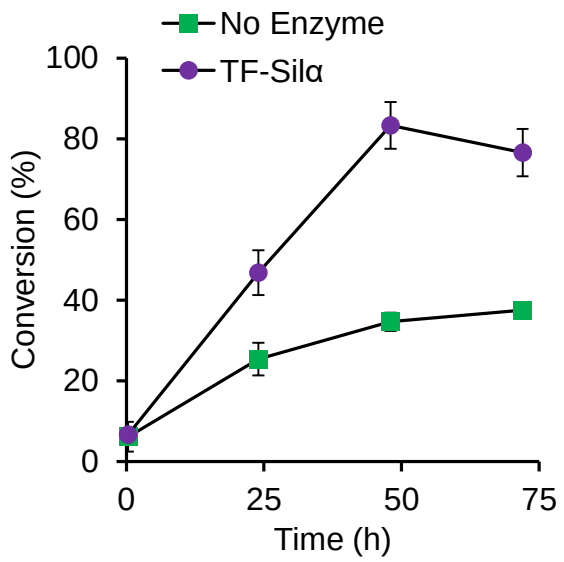

Figure S23. Graph of percentage conversion to silyl ether **16** against reaction time from silylation with **10**, as determined by GC-MS analysis of the reaction products.

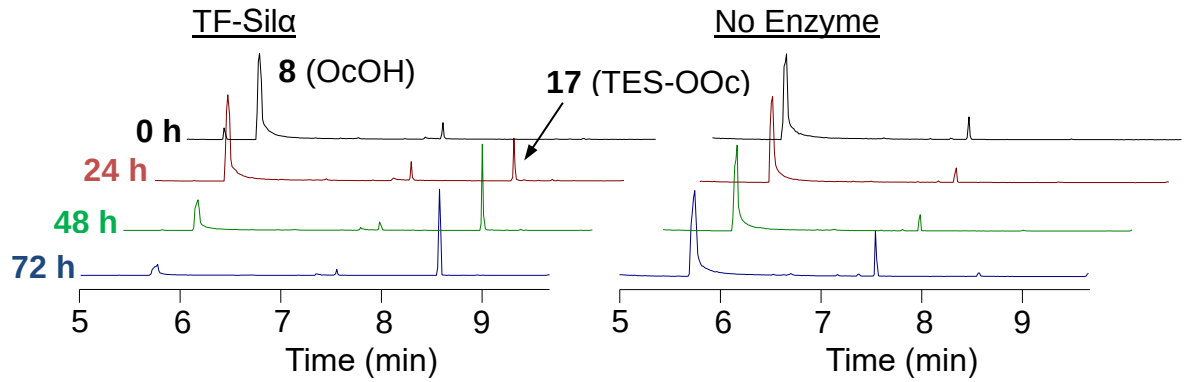

Figure S24. The GC chromatograms for the condensation of **17** from **8** and **11** using optimized conditions (75 °C, lyoprotectants added)**.**

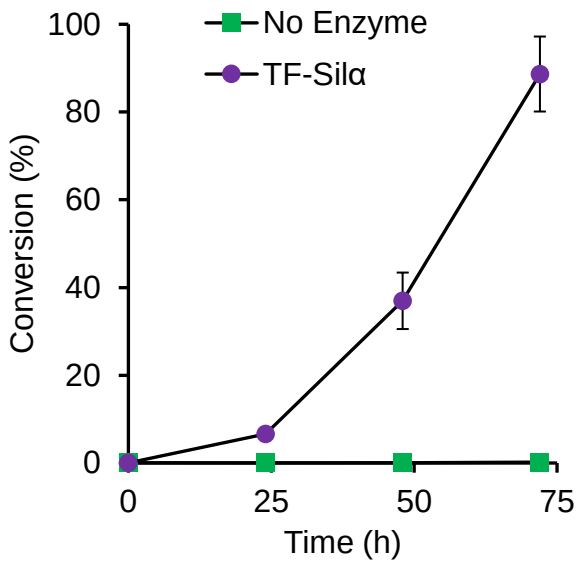

Figure S25. Graph of percentage conversion to silyl ether **17** against reaction time from silylation with **11**, as determined by GC-MS analysis of the reaction products.

1.8 Silyl transetherification reactions

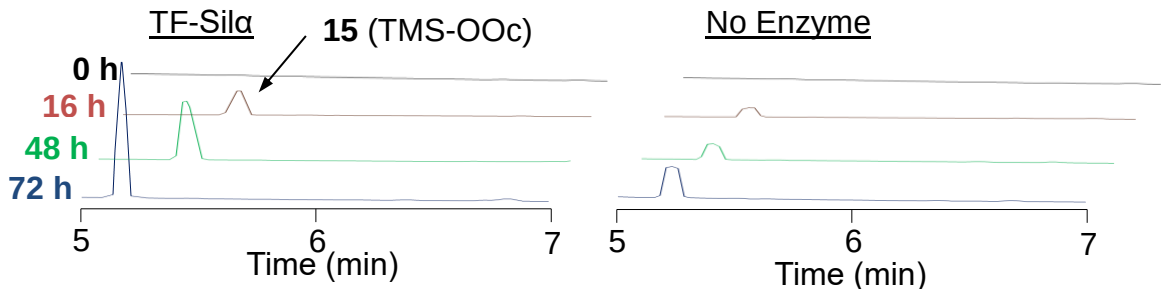

Figure S26. The GC chromatograms for the formation of **15** by transetherification from ethoxysilane **12** to **8**.

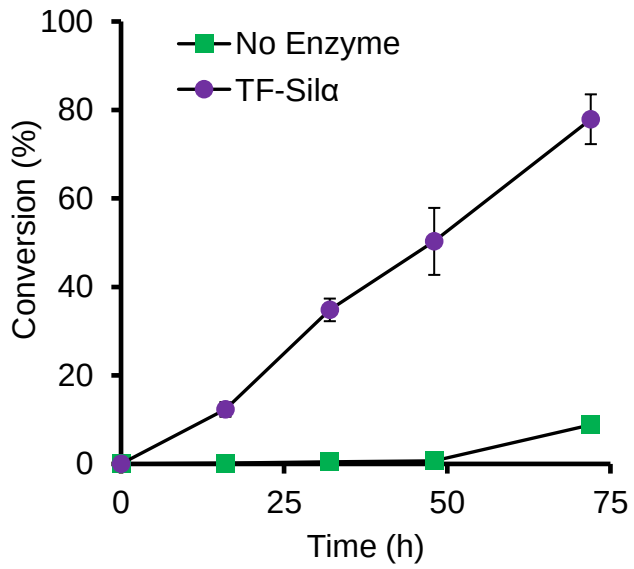

Figure S27. Graph of percentage conversion to silyl ether **15** against reaction time from transetherification with **12**, as determined by GC-MS analysis of the reaction products.

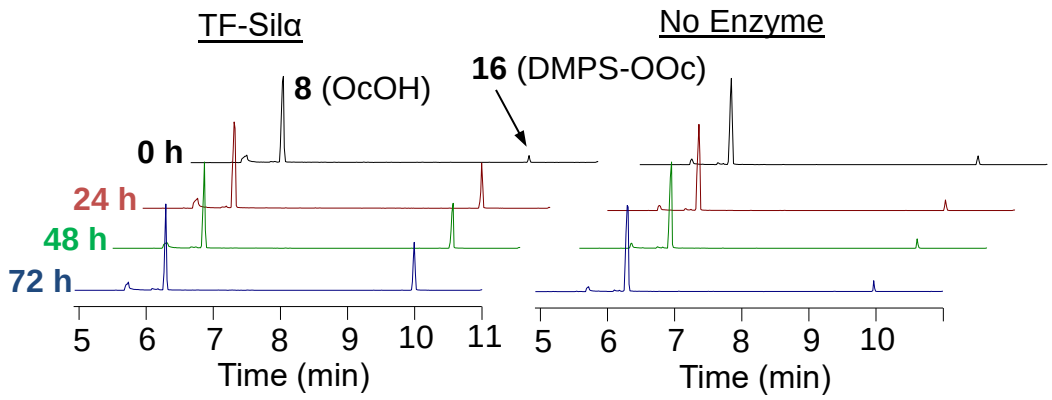

Figure S28. The GC chromatograms for the formation of **16** by transetherification from ethoxysilane **13** to **8**.

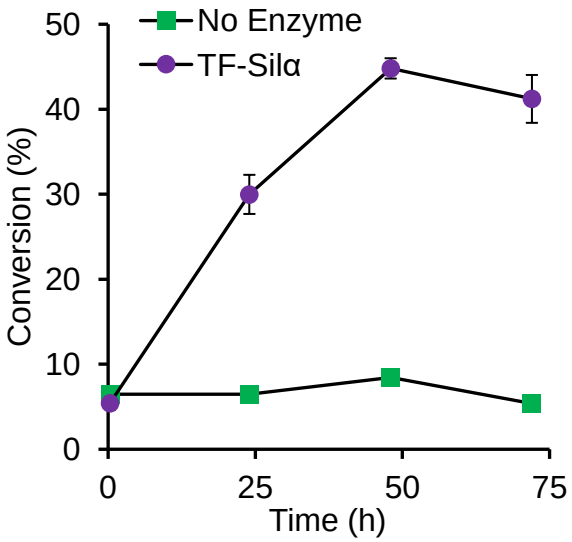

Figure S29. Graph of percentage conversion to silyl ether **16** against reaction time from transetherification with **13**, as determined by GC-MS analysis of the reaction products.

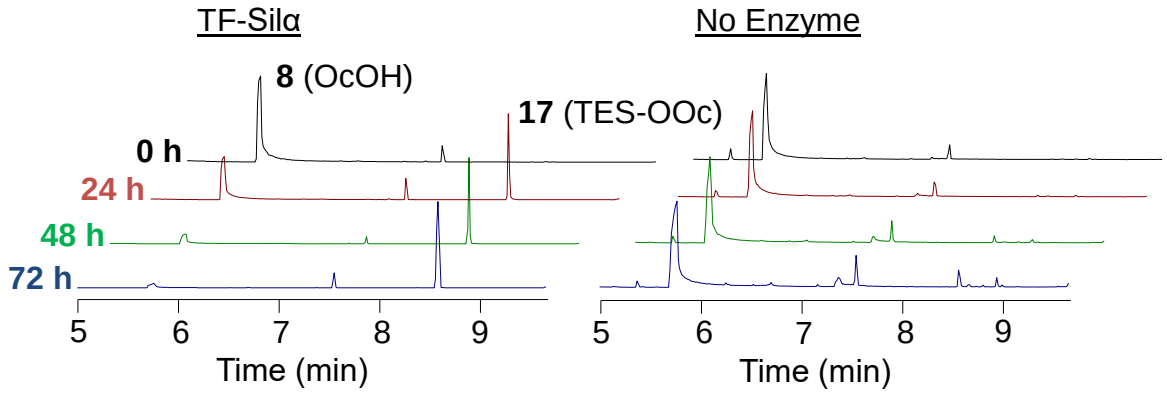

Figure S30. The GC chromatograms for the formation of **17** by transetherification from ethoxysilane **14** to **8**.

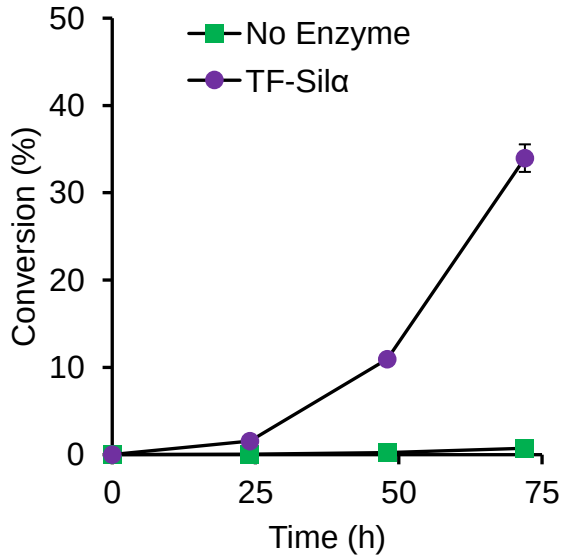

Figure S31. Graph of percentage conversion to silyl ether **17** against reaction time from transetherification with **14**, as determined by GC-MS analysis of the reaction products.

1.9 Regioselectivity of silylation.

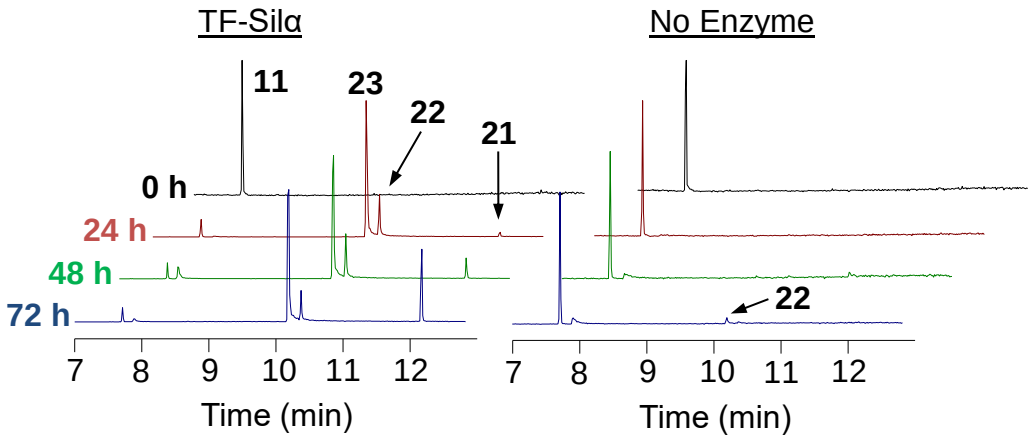

Figure S32. The GC chromatograms of the silylation of **18** with **11** to give **21**–**23**.

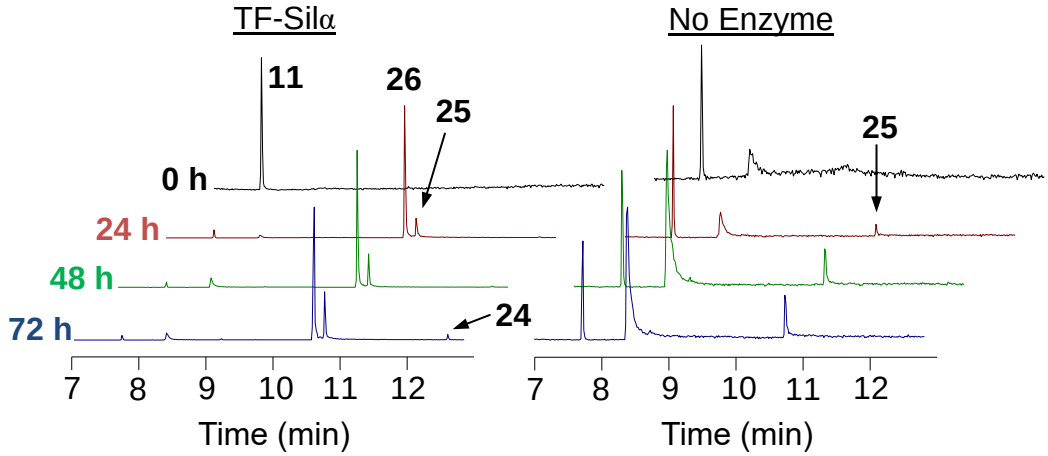

Figure S33. The GC chromatograms of the silylation of **19** with **11** to give **24**–**26**.

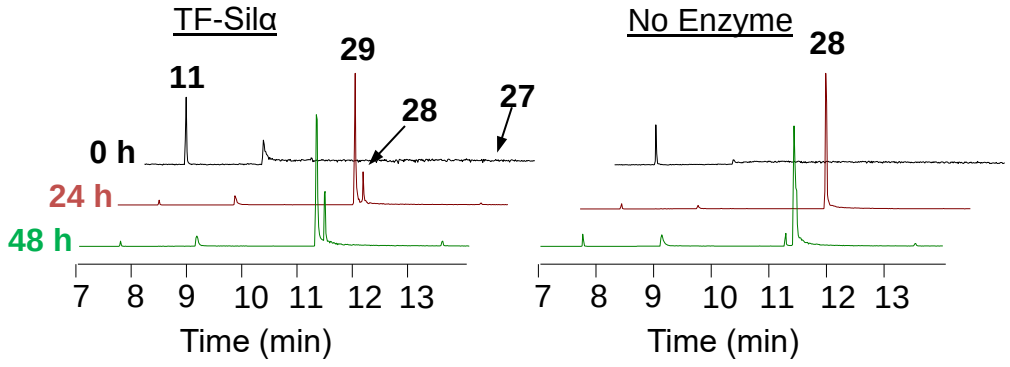

Figure S34. The GC chromatograms of the silylation of **20** with **11** to give **27**–**29**.

1.9.1 Confirmation of Regioisomer Identity

The structural identity of the products **19**-**29** was based upon a comparison of the spectroscopic data reported in the literature (for **21**, **22**, **23**, **24**, **26**, **27**, **28**)(1-3) and by the correlation of spectroscopic data (^{1}H NMR, ^{13}C NMR, IR) when this data was not available in the literature.

In those cases where spectroscopic data was not available for direct comparison, correlations were based upon a detailed analysis of the NMR spectra of this library of compounds. Specifically, the well-documented observation(4-6) that the δ_C of carbon atoms *ortho*- to a phenol experience a 5 ppm increase when converted to simple alkylsilyl ethers.

Hence, in the case of **23**, **26** and **29** (phenolic silylation) the δ_C of the *ortho*-carbons are observed at ~120 ppm (Table S4). In contrast, with **22**, **25** and **28** (aliphatic alcohol silylated, phenol free) the corresponding resonance lies at ~115 ppm. These observations were also consistent with the 4-nitrophenoxy substrates **1**-**3** (Table S5) and other similar molecules that have been reported in the literature.(1, 2) Furthermore, an independent in-house synthesis of **23** by an unambiguous route (see section 2.7.9)(2) gave a resonance at δ 121.2 ppm for the corresponding carbon atom, further confirming the NMR spectroscopic assignments.

Finally, the FT-IR spectra of compounds **21, 22, 24, 25, 27** and **28** all contained two strong absorptions in the range of 1000-1100 cm^{-1} (Table S4) that can be assigned to the Si–O bond of the aliphatic silyl ether.(7) The compounds bearing only aryl silyl ethers **24**, **27** and **29**, show no such absorption in this region but instead show the Si–O absorption at ~1250 cm^{-1}.

Table S4. Table of ^{13}C NMR chemical shifts of *ortho* positions (positions C^2 and C^6) for compounds **21-29**.

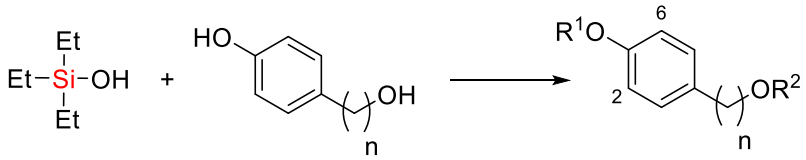

11 **18-20** **21-29**

Substrate	Product	R^1	R^2	n	NMR δ_C of *ortho* positions, ppm	IR wavenumber(s) of Si–O stretch, cm^{-1}
18	**21**	TES	TES	1	120.7	1003, 1081, 1257
18	**22**	H	TES	1	115.6	1002, 1082
18	**23**	TES	H	1	121.2	1257
19	**24**	TES	TES	2	120.6	1004, 1091, 1257
19	**25**	H	TES	2	115.7	1003, 1084
19	**26**	TES	H	2	121.1	1257
20	**27**	TES	TES	3	120.2	1004, 1095, 1257
20	**28**	H	TES	3	115.6	1004, 1094
20	**29**	TES	H	3	120.4	1256

Table S5. Table of ^{13}C NMR chemical shifts of *ortho* positions (positions C^2 and C^6) in 4-nitrophenol and compounds **1-3**.

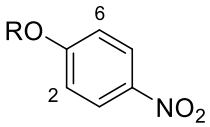

Compound	**R**	NMR δ_C of *ortho* positions, ppm
HONp	H	115.8[a]
1	TBDMS	120.1
2	TDS	122.5
3	TIPS	119.9

[a] Data from ref. (2)

1.10 Comparisons between Biocatalysis and Small Molecule Catalysis

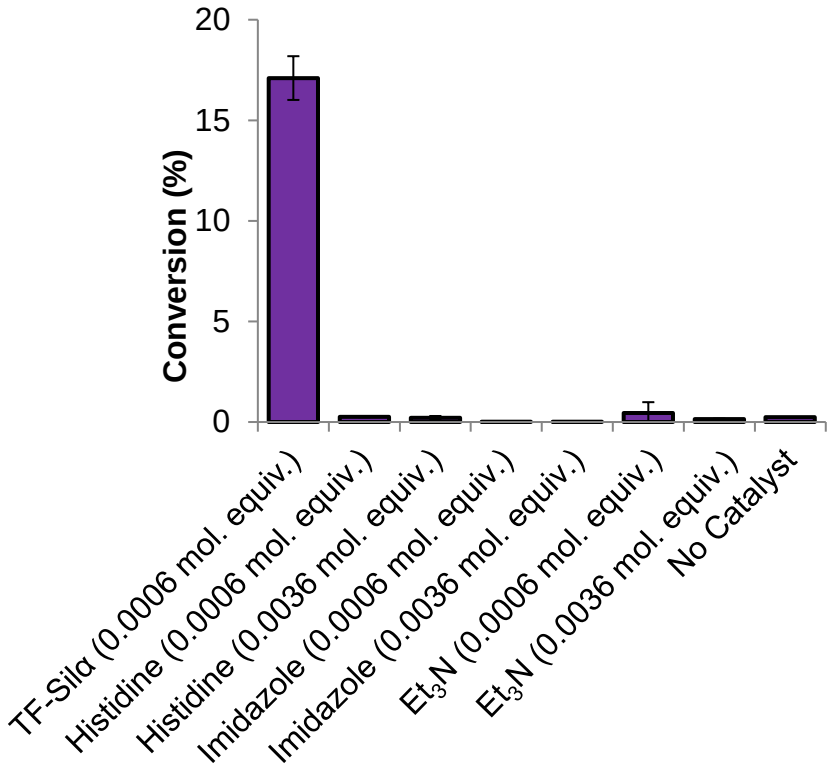

Figure S35. Graph of percentage conversion of **15** from **8** and **9** after 24 h using the same conditions as comparing the different catalysts.

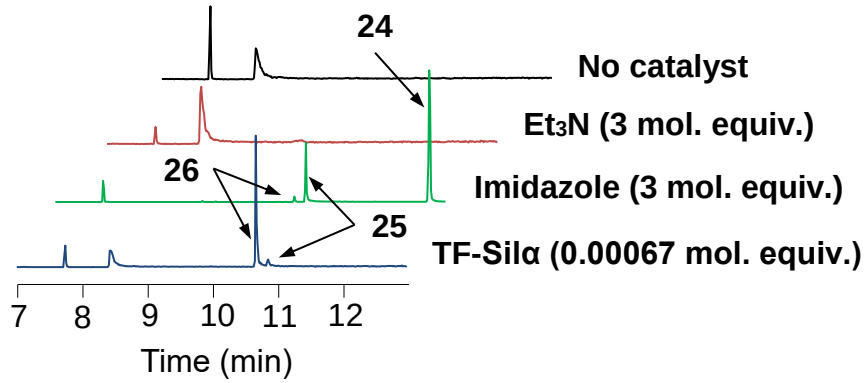

Figure S36. The GC chromatograms of the silylation of **19** with **11** to give **24–26** comparing TF-Silα, imidazole and trimethylamine as catalysts after a 5 h reaction time. For the reactions catalyzed by TF-Silα and imidazole, the relative ratios of compounds **24**:**25**:**26** are ~1:13:86 and 74:24:2, respectively. No significant conversions were detected when Et_3N was used or if no bases were added.

2 Materials and Methods.

2.1 Materials and equipment.

All chemical reagents were purchased from either Sigma-Aldrich, VWR or Fisher Scientific. The silicomolybdic acid assay kit was purchased from VWR (catalogue no: 1.14794.0001). All molecular cloning enzymes were acquired from New England Biolabs. The synthetic DNA encoding the silα gene was produced by GenScript (Piscataway, NJ). The vectors coding for the fusion proteins were pET28a-GST (Novagen), pHis-Trx Plasmid (Manchester Protein Production Facility, UK), pOPINM, pOPINS (both from Oxford Protein Production Facility, UK) and pColdTF (TaKaRa Bio, Kyoto, Japan); for glutathione-*S*-transferase, thioredoxin, SUMO, maltose binding protein and trigger factor, respectively. The *E. coli* strains used were BL21 (DE3) (Novagen), Origami (DE3) (Novagen) and ArcticExpress (DE2) (Agilent).

Immobilized metal affinity chromatography (IMAC) was performed with NTA-agarose gel from QIAGEN (Hilden, Germany) and size exclusion chromatography (SEC) with a HiLoad 16/600 Superdex 200 pg column from GE Healthcare. The non-denaturing polyacrylamide gel electrophoresis was carried out with Mini-PROTEAN TGX Stain-Free precast 10% polyacrylamide gels (Bio-Rad) in standard Tris/glycine running buffer, with PageRuler Plus Prestained Protein Ladder protein size markers (Thermofisher).

The UV-Vis/colorimetric assays were performed in a quartz 96-well microtitre plate (Hellma Analytics, Müllheim, Germany) on a BioTek Synergy HT multi-mode reader. GC-MS analyses were performed according to the details in Table S6, except for the condensation of **12** to **15**, which is detailed in Table S7.

Table S6. GC-MS experimental parameters.

Parameter	Setting
Instrument	Thermo Finnigan PolarisQ Ion Trap Mass Spectrometer
Carrier gas	99.9995% Ultra high purity (UHP) helium
GC inlet, split	200 °C, split flow 10 (min mL^{-1}), split ratio 10
Detector	PolarisQ positive ion source (260 °C), full scan (35-650 amu), 0.59 scan/s
MS ionization	Electron ionization
GC temperature program	60 (2 min) → 250 (4 min) at 20 °C min^{-1}, 15 min total run time
GC column	Thermo Scientific TraceGold TG-1MS (30 m × 0.25 mm, 0.25 μm film)
GC transfer line temperature	275 °C
Volume injected	1 μL

Table S7. GC-MS experimental parameters.

Parameter	Setting
Instrument	Varian Saturn 2000 Ion Trap Mass Spectrometer
Carrier gas	99.998% Ultra high purity (UHP) helium
GC inlet, split	200 °C, split flow 10 (min mL^{-1}), split ratio 10
Detector	Saturn 2000 positive ion source (260 °C), full scan (35-650 amu), 0.59 scan/s
MS ionization	Electron ionization
GC temperature program	60 (2 min) → 250 (4 min) at 20 °C min^{-1}, 15.5 min total run time
GC column	Zebron ZB-Semi Volatiles (30 m × 0.25 mm, 0.25 μm film)
GC transfer line temperature	275 °C
Volume injected	1 μL

2.2 Gene cloning and protein overexpression.

The codon optimized DNA construct corresponding to the mature form of silicatein-α from *S. domencula* was cloned into an in-house pHis vector (University of Manchester Protein Expression Facility). For cloning into other vectors, the silα gene was then amplified by PCR using the primers:

Forward (with XhoI restriction site): AAAAAACTCGAGGACTATCCGGAAGCCGTTGA

Reverse (with EcoRI restriction site): AAAAAAGAATTCTTACAGGGTCGGATAGCTGG

The vectors and the PCR fragments were digested with the XhoI and EcoRI restriction enzymes and ligated overnight at 16°C, resulting in the insertion of the gene fragment in frame with the fusion protein genes. Successful cloning was confirmed by DNA sequencing. All vectors used contained an upstream T7 promoter, which is compatible with *E. coli* BL21(DE3) strains that produce T7 RNA polymerase upon induction with isopropyl β-D-1-thiogalactopyranoside (IPTG). The vectors were then transformed into chemically competent cells of the various *E. coli* strains.

For the production of the Silα enzyme, BL21(DE3) cells transformed with pHis-silα were grown at 37 °C overnight, with relevant antibiotics (ampicillin). This resulting culture (5ml) was used to inoculate 1 L culture LB medium that was grown at 37 ºC to reach the optical density (A_{600}) of 0.5, upon which 1mM IPTG was added and the culture and shaken overnight at 37 ºC. The cells were precipitated by centrifugation (4500 g for 20 min), the media decanted and the cells resuspended in lysis buffer containing surfactants (1 % v/v Triton X-100, 5 mM CHAPS, 20 mM Tris, pH 7.5). The resuspended cells were lysed by sonication, the lysate centrifuged and the supernatant collected. The protein was then isolated from the supernatant by IMAC using a slow elution through a gravity flow column containing 5 mL of gel, followed by SEC with 500 mM NaCl, 100 mM potassium phosphate buffer, pH 7.5.

For TF-Sil, the protein was successfully isolated from *E. coli* BL21(DE3) cells transformed with pColdTF-silα and cultured according to previously reported conditions.(8) The cells were harvested as above and re-suspended in lysis buffer (100 mM potassium phosphate buffer, pH 8.0). The mixture lysed by sonication and purified by IMAC and SEC as above.

In all cases, the chromatography fractions containing the purified enzyme (as identified by SDS-PAGE) were combined and buffer exchanged by overnight dialysis into 100 mM NaCl, 50 mM Tris, pH 8.5.

2.2.1 Molecular cloning of Ser_{26}Ala mutant.

The desired mutation was inserted into the pColdTF-silα vector by the overlap extension method(9) using the following primers:

Non-mutagenic forward primer: `CCACGCGGTAGTGGTGGTATC`

Non-mutagenic reverse primer: `TACCTATCTAGACTGCAGGTC`

Mutagenic forward primer: `GGGGCCGCATATGCTTTTTCT`

Mutagenic reverse primer: `AGAAAAAGCATATGCGGCCCC`

The gene mutation was confirmed by DNA sequencing. The mutant protein was then produced using the same procedures as TF-Silα as noted above.

2.3 Circular Dichroism (CD) Spectroscopy.

The spectra were recorded using a Chirascan CD Spectrometer (Applied Photophysics Limited, UK). Quartz cells with 0.1 mm pathlength (Starna Scientific, UK) were used for all measurements. Data was collected over a wavelength range of 190 to 260 nm, at a scan speed of 0.5 nm s^{-1}. The temperature was maintained at 22°C using a temperature controlled chamber. Each protein was analysed in buffered solution (50 mM Tris, 100 mM NaCl, pH 8.5) with baseline measurements using buffer alone. In all cases, the proteins were analysed at a concentration of 9.5 mM. An averaged spectrum of each sample was obtained by 20 repeat scans and subtraction of the mean baseline. The raw CD data was then used to calculate the ME and MRE. The secondary structure content of each protein was estimated with the CDNN circular dichroism algorithm,(10) using the ME data.

The theoretical values for TF-Silα secondary structure prediction in Table S3 were calculated using SWISS-MODEL and Swiss PdbViewer.(11) The data was obtained using the values given in PDBsum (www.ebi.ac.uk/pdbsum/) for Trigger factor (PDB ref. 1w26) and a homology model constructed using cathsilicatein (PDB ref. 2vhs) for silicatein separately. The theoretical percentage values for each secondary structure in TF-Silα were then calculated from these separate values as a proportion of their relative molecular weight in the fusion protein.

2.4 Assays of enzymatic silica formation

In all cases the either Silα or TF-Silα (500 μL, 2.7 μM) was used in a buffered solution (100 mM NaCl, 50 mM Tris) that was adjusted to the relevant pH (see below). As controls, the enzyme solution was heated to 85 °C for 10 min to obtain the heat denatured enzyme, which was allowed to cool to room temperature prior to use. All reactions were performed in triplicate.

2.4.1 Enzyme assays using TEOS

TEOS (0.5 mmol, 111 μL) was added to the enzyme solution (adjusted to pH 8.0) and thoroughly mixed to obtain a uniform suspension. These suspensions were shaken at 22 °C for 1 h, centrifuged (13000 g for 30 min) and the supernatant discarded. The precipitated silica was washed with EtOH (4 × 200 μL) and 2M NaOH solution (to a final volume of 500 μL) added to hydrolyze the silica. The quantity of silicon in this solution of monomeric sodium silicate was then quantified using the silicomolybdic acid assay kit according to the manufacturer's instructions. This assay was calibrated (Figure S5C) with a standard solution of Na_2SiF_6 (0.960 g L^{-1} , equivalent to 5 μg mL^{-1} of silica).(12-14)

2.4.2 Enzyme assays using silicic acid

The silicic acid solutions were produced by acidic hydrolysis of TEOS according to previously described methods.(15, 16) This solution (5 mM, 10 μL) was added to the enzyme solution (adjusted to pH 7.0) and thoroughly mixed. This reaction mixture was then shaken for at 22 °C for 1 h. Subsequently, the silica was isolated and quantified in the same manner as above.

2.5 Colorimetric 4-nitrophenol silyl ether hydrolysis assays

1 mM stock solutions were prepared of the 4-nitrophenoxysilanes (**1**–**3**), 4-nitrophenyl ester (**31**) or 4-nitrophenylamides (**7** or **32**) in buffer (100mM NaCl, 50mM Tris, adjusted to the relevant pH for the experiment), with 10 % v/v 1,4-dioxane to aid solubility. Aliquots of these stock solutions were pipetted into each well of the microtitre plate and made up to a final volume of 100 μL by addition of the appropriate volume of the same buffer/dioxane solution (adjusted to the relevant pH) to give the desired concentrations of substrates. 100 μL solutions of the relevant enzyme at the desired concentration were then added to each well immediately prior to the commencement of spectrophotometric data collection. The UV-Vis absorbance was measured at 405 nm at suitable time intervals with the plate shaken continuously at 22 °C throughout the duration of the data collection.

Quantification of the released 4-nitrophenol or 4-nitroaniline was based on calibrations using known amounts of these compounds dissolved in buffer (5 % v/v dioxane, 100 mM NaCl, 50 mM Tris), adjusted to the relevant pH (Figures S6 and S7).

All reactions were performed in triplicate, and the error bars presented in the graphs refer to the standard deviation of these three independent measurements for each data point.

To calculate the Michaelis-Menten constants, the time course data for each experiment was averaged. The initial velocities obtained from the tangent of the growth curve as close as possible to its origin. The linear regression technique used to obtain the tangent of this slope. The velocity and corresponding substrate concentration data was then processed with the algorithm for the Michaelis-Menten model of enzyme kinetics within the SigmaPlot 12.0 software to obtain the K_M and k_{cat} values.

2.6 Enzymatic reactions in organic solvents

To produce the enzyme preparations used in organic solvents, the buffer in enzyme solutions from section 2.2 are exchanged by repeated centrifugal ultrafiltration into either 100 mM ammonium carbonate (at the appropriate pH for the pH survey experiment) or 100 mM potassium phosphate buffer (pH 7.0 for all other experiments) with 20 mM KCl, and the final volume and enzyme concentration adjusted to 5 mL and 5 mg mL^{-1}. 18-Crown-6 (2 mM in H_2O, 100 μL) is added where necessary for that particular experiment, the mixture was flash frozen in liquid nitrogen and lyophilized. Materials for the negative control experiments were prepared by lyophilizing the above buffer mixture without the enzyme.

2.6.1 Silyl etherifications and transetherifications with 1-octanol

The lyophilized solids are resuspended in *n*-octane (5 mL) and OcOH (0.2 mL, 1.26 mmol) was added, followed by the respective silanol or ethoxysilane (6.30 mmol, 5 mol. eq. relative to OcOH). The stirred reaction mixture was adjusted to the relevant temperature and aliquots (100 μL) of the reaction mixture were removed at 24 h intervals. These aliquots were each centrifuged (13000 g for 3 min) to remove the solids and the supernatant analyzed by GC-MS (duplicate run and randomized order). Each reaction was performed in triplicate, and the error bars presented in the graphs refer to the standard deviation of these three independent measurements for each data point. For quantification of conversation rates, the GC-MS was first calibrated using authentic samples of **15**–**17** that were chemically synthesized (see below).

2.6.2 Silyl etherifications to 4-(ω-hydroxyalkyl)phenols catalyzed by TF-Silα

The lyophilized solids are resuspended in *n*-octane (5 mL) and the relevant diol (1.26 mmol) followed by TES-OH (968 μL, 5 mol. eq. relative to diol) were added. The stirred reaction mixture was heated to 75 °C and aliquots (100 μL) of the reaction mixture were removed at 24

h intervals. These aliquots were processed and analyzed as above using authentic samples of **21-29** that were chemically synthesized (see below).

2.6.3 Silyl etherifications to 4-(ω-hydroxyalkyl)phenols catalyzed by small molecules

The imidazole, Et_3N or histidine (at the relevant mol. eq. relative to diol) was suspended in *n*-octane (5 mL) and the relevant diol (1.26 mmol) and TES-OH (968 μL, 5 mol. eq. relative to diol) added. The stirred reaction mixture was heated to 75 °C and aliquots (100 μL) of the reaction mixture were removed at 24 h intervals. Each aliquot was each filtered to remove any solids and the filtrate analyzed by GC-MS as noted above. Each reaction was performed in triplicate.

2.7 Synthesis of enzyme substrates

2.7.1 *tert*-Butyldimethyl(4-nitrophenoxy)silane, TBDMS-ONp, 1

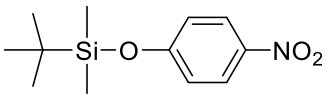

To a solution of 4-nitrophenol (1150 mg, 8.22 mmol) in anhydrous DMF (10 mL) was added *tert*-butylchlorodimethylsilane (1250 mg, 8.22 mmol) followed by imidazole (1125 mg, 16.58 mmol). The reaction mixture was stirred for 16 h, after which hexane (10 mL) was added and the organic phase washed with H_2O (10 mL). The organic phase was then dried with $MgSO_4$ and concentrated under reduced pressure. The residue was purified by silica gel chromatography using the eluent noted below to yield the desired **1** as a white solid (1526 mg, 73%); R_f 0.41 (EtOAc:hexane, 1:20); ν_{max} (solid)/cm^{-1} 2954 (C-H); 1589 (NO_2), 1277 (SiOAr), 1110 (C-O), 903 (Si-C); δ_H (400 MHz; $CDCl_3$) 8.16 (d, *J* 9.2 Hz, 2H), 6.90 (d, *J* 9.2 Hz, 2H), 1.08 (s, 9H), 0.28 (s, 6H); δ_C (100 MHz; $CDCl_3$) 161.6, 141.9, 125.8, 120.1, 25.5, 18.2, –4.3; MS *m/z* (ES^+) 254 (100 %, $[M+H]^+$); HRMS *m/z* (ES^+); Calcd. for $C_{12}H_{20}NO_3Si$ $[M+H]^+$: 254.1207, found: 254.1196.

2.7.2 Dimethylthexyl(4-nitrophenoxy)silane, TDS-ONp, 2

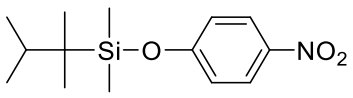

To a solution of 4-nitrophenol (353 mg, 2.54 mmol) in anhydrous DMF (5mL) was added chlorodimethylthexylsilane (0.5 mL, 2.54 mmol) and imidazole (345 mg, 5.08 mmol). The reaction mixture stirred for 16 h, after which hexane (10 mL) was added and the organic phase washed with H_2O (10 mL). The organic phase was then dried with $MgSO_4$ and concentrated under reduced pressure. The residual oil was purified by silica gel chromatography using the eluent noted below to yield **2** as a colorless oil (693 mg, 97%); R_f 0.43 (EtOAc:hexane, 1:20); ν_{max} (oil)/cm^{-1} 2957 (C-H), 1495 (NO_2), 1276 (SiOAr), 1110 (C-O), 901(Si-C); δ_H (400 MHz; $CDCl_3$) 8.16 (d, *J* 9.1 Hz, 2H), 6.89 (d, *J* 9.1 Hz, 2H), 1.73–1.76 (m, 1H), 0.95–0.97 (m, 12H), 0.31 (s, 6H); δ_C (100 MHz; $CDCl_3$) 163.8, 144.2, 128.2, 122.5, 36.4, 27.5, 22.4, 20.9, 0.0; MS *m/z* (ES^+) 282 (100 %, $[M+H]^+$); HRMS *m/z* (ES^+) Calcd. for $C_{14}H_{24}NO_3Si$ $[M+H]^+$: 282.1520, found: 282.1517.

2.7.3 Triisopropyl(4-nitrophenoxy)silane, TIPS-ONp, 3

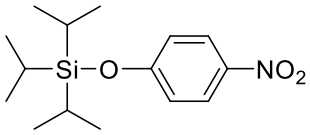

To a solution of 4-nitrophenol (258 mg, 1.86 mmol) in anhydrous DMF (15 mL) was added triisopropylsilyl trifluoromethanesulfonate (0.5 mL, 1.86 mmol) and Et_3N (0.51 mL, 3.72 mmol). The reaction mixture stirred for 16 h, after which hexane (200 mL) was added and the organic phase washed with H_2O (200 mL). The organic phase was then dried with $MgSO_4$ and concentrated under reduced pressure. The residual oil was purified by silica gel chromatography using the eluent noted below to yield **3** as a colorless oil (437 mg, 79%); R_f 0.56 (EtOAc:hexane, 1:20); ν_{max} (oil)/cm^{-1} 2866 (C-H), 1512 (NO_2), 1279 (SiOAr), , 1110 (C-O), 903 (Si-C); δ_H (400 MHz; $CDCl_3$) 8.15 (d, *J* 9.2 Hz, 2H), 6.93 (d, *J* 9.2 Hz, 2H), 1.27–1.35 (m, 3H), 1.13 (d, *J* 7.2 Hz, 18H); δ_C (100 MHz; $CDCl_3$) 162.0, 141.7, 125.8, 119.9, 17.7, 12.6;

MS *m/z* (ES^+) 296 (100 %, $[M+H]^+$); HRMS *m/z* (ES^+) Calcd. for $C_{15}H_{26}NO_3Si$ $[M+H]^+$: 296.1676, found: 296.1673.

2.7.4 Trimethyl(octyloxy)silane, TMS-OOc, 15

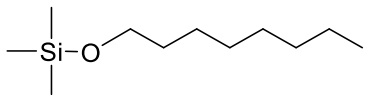

To a solution of hexamethyldisilazane (3 mL, 19.15 mmol) and 1-octanol (0.5 mL, 3.83 mmol) was added trifluoroacetic acid (1.5 mL, 19.15 mmol) dropwise over 10 min and the mixture stirred for 1 h. The reactants were removed by evaporation (153 °C, 80 mbar) to yield **15** as a colorless oil that was pure by NMR analysis (150 mg, 19%); ν_{max} (oil)/cm^{-1} 2926 (C-H), 1094 (Si-O), 836 (Si-C); δ_H (400 MHz; $CDCl_3$) 3.58 (t, *J* 6.7 Hz, 2H), 1.52–1.56 (m, 2H), 1.29–1.34 (m, 10H), 0.90 (t, *J* 6.8 Hz, 3H), –0.13 (s, 9H); δ_C (100 MHz; $CDCl_3$) 62.7, 32.7, 31.8, 29.4, 29.3, 25.8, 125.1, 22.6, 14.1, –0.4; MS *m/z* (EI) 187 (100%, $[M^+$-Me]); HRMS *m/z* (APCI) Calcd. for $C_{11}H_{27}OSi$ $[M+H]^+$: 203.1830, found: 203.1826.

2.7.5 Dimethylphenyl(octyloxy)silane, DMPS-OOc, 16

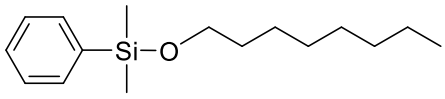

To a solution of Et_3N (0.78 mL, 5.85 mmol) in anhydrous DMF (5 mL) was added chlorodimethylphenylsilane (0.5 mL, 2.92 mmol) followed by 1-octanol (0.95 mL, 5.85 mmol) and stirred the mixture stirred for 3 h. The reactants were removed by evaporation (160 °C, 80 mbar) to yield **16** as a pale yellow oil that was pure by NMR analysis (420 mg, 54%); ν_{max} (oil)/cm^{-1} 2955 (C-H), 826 (Si-O), 697 (Si-C); δ_H (400 MHz; $CDCl_3$) 7.55–7.61 (m, 2H), 7.37–7.41 (m, 3H), 3.66 (t, *J* 6.7, 1H), 3.61 (t, *J* 6.6,1H), 1.53–1.57 (m, 2H), 1.27–1.32 (m, 10H), 0.88–0.92 (m, 3H), 0.40 (s, 3H), 0.35 (s, 3H); δ_C (100 MHz; $CDCl_3$) 139.4, 137.6, 133.4, 132.9, 129.4, 129.2, 127.6, 63.1, 33.3, 32.6, 31.8, 29.2, 25.7, 22.6, 14.1, 0.8, –1.7; MS *m/z* (APCI) 265 (100%, $[M+H]^+$), HRMS *m/z* (APCI) Calcd. for $C_{16}H_{29}OSi$ $[M+H]^+$: 265.1982, found: 265.1981.

2.7.6 Triethyl(octyloxy)silane, TES-OOc, 17

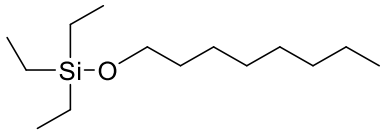

To a solution of Et_3N (0.5 mL, 5.2 mmol) in anhydrous DMF (5 mL) was added chlorotriethylsilane (0.5 mL, 2.65 mmol) followed by 1-octanol (0.84 mL, 5.2 mmol) and stirred for 3h. Hexane (50 mL) was added to the reaction mixture and the organic phase washed with H_2O (50 mL). The organic phase was then dried with $MgSO_4$ and concentrated under reduced pressure. The residue was purified by silica gel chromatography using the eluent noted below to yield **17** as a colorless oil (530 mg, 82%); R_f 0.44 (hexane:EtOAc, 1:20); ν_{max} (oil)/cm^{-1} 2925 (C-H), 1096 (Si-O), 723 (Si-C); δ_H (400 MHz; $CDCl_3$) 3.61 (t, *J* 6.7 Hz, 2H), 1.52–1.56 (m, 2H), 1.30-1.29 (m, 10H), 0.98 (t, *J* 7.9 Hz, 9H), 0.62 (q, *J* 8.0 Hz, 6H); δ_C (100 MHz; $CDCl_3$) 32.9, 31.8, 29.4, 29.31, 25.8, 22.6, 14.0, 6.7, 4.4; MS *m/z* (APCI) 245 (100 %, $[M+H]^+$); HRMS *m/z* (APCI) Calcd. for $C_{14}H_{33}OSi$ $[M+H]^+$: 245.2295, found: 245.2294.

2.7.7 Triethyl((4-((triethylsilyl)oxy)benzyl)oxy)silane, 21

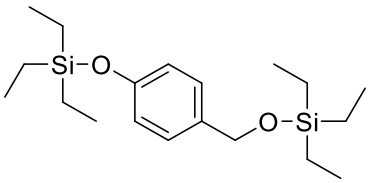

To a solution of 4-hydroxybenzyl alcohol (440 mg, 3.6 mmol) in anhydrous DMF (15 mL) was added chlorotriethylsilane (1.2 mL, 7.2 mmol) followed by Et_3N (1 mL, 7.2 mmol) and the mixture stirred for 16 h. Hexane (200 mL) was added to the reaction mixture and the organic phase washed with H_2O (200 mL). The organic phase was then dried with $MgSO_4$ and concentrated under reduced pressure. The residue was purified by silica gel chromatography using the eluent noted below to yield **21** as a colorless oil (243 mg, 19 %); R_f 0.75 (EtOAc:hexane 2:1); ν_{max} (oil)/cm^{-1} 2910 (CH), 1508 (C-C), 1257 (Ar-O), 1081 ($SiOCH_2$), 906 (SiOAr), 726 ($SiC(C_2H_3)_3$); δ_H (400 MHz; $CDCl_3$) 7.19 (d, , *J* 8.6 Hz, 2H), 6.82 (d, *J* 8.5 Hz, 2H), 4.63 (s, 2H), 0.92 (t, *J* 6.4 Hz 9H), 0.88 (t, *J* 6.4 Hz 9H), 0.66 (q, *J* 7.7 Hz, 6H), 0.56 (q, *J* 7.9 Hz, 6H); δ_C (100 MHz; $CDCl_3$) 156.0, 135.2, 128.9, 120.8, 65.1, 6.8, 6.7, 5.0, 4.6; MS

m/z (APCI) 351 (100%, $[M–H]^-$), HRMS *m/z* (APCI) Calcd. for $C_{19}H_{36}O_2Si_2Na$ $[M+Na]^+$: 375.2146, found: 375.2133

2.7.8 4-(((Triethylsilyl)oxy)methyl)phenol, 22

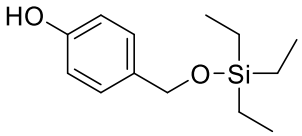

Compound **22** was isolated as a pale yellow oil from the same reaction mixture as **21** during column chromatography (153 mg, 17%); R_f 0.51 (hexane:EtOAc, 2:1); ν_{max} (oil)/cm^{-1} 3308 (OH), 2910 (CH), 1236 (ArO), 1002 ($SiOCH_2$), 741 ($Si(C_2H_3)_3$); δ_H (400 MHz; $CDCl_3$) 7.20 (d, *J* 8.6 Hz, 2H), 6.79 (d, *J* 8.5 Hz, 2H), 4.62 (s, 2H), 0.88 (t, *J* 7.5 Hz, 9H), 0.57 (q, *J* 7.2 Hz, 6H); δ_C (100 MHz; $CDCl_3$) 155.4, 134.3, 128.7, 115.6, 64.8, 6.8, 4.5; MS *m/z* (APCI) 221.1 (100%, $[M–OH]^+$); HRMS *m/z* (APCI) Calcd for $C_{13}H_{21}OSi$ $[M–OH]^+$: 221.1356, found: 221.1355.

2.7.9 (4-((Triethylsilyl)oxy)phenyl)methanol, 23 (1)

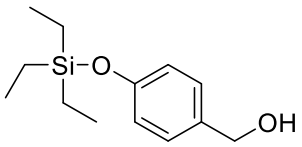

To a solution of 4-hydroxybenzaldehyde (1 g, 8.1 mmol) in anhydrous CH_2Cl_2 (15 mL) was added imidazole (1 g, 14.7 mmol), followed by portionwise addition of chlorotriethylsilane (1.5 mL, 8.8 mmol) and the mixture stirred for 4 h at room temperature. The mixture was then filtered through Celite. The solvent was removed under reduced pressure to obtain the crude product as a white solid (2.70 g). This solid was dissolved in MeOH (15 mL) at 0 °C and $NaBH_4$ (400 mg, 10.5 mmol) was added portionwise. After completion of addition, the mixture stirred at room temperature for 1 h. The MeOH evaporated under reduced pressure, the residue was resuspended in potassium phosphate buffer (pH 7.5, 0.5 M, 50 mL) and extracted with CH_2Cl_2 (3 x 100 mL). The organic phase was dried with $MgSO_4$, concentrated under reduced pressure and the residue was purified by silica gel chromatography using the eluent noted

below to yield **23** as a colorless oil (523 mg, 27%); R_f 0.37 (hexane:EtOAc, 2:1); ν_{max} (oil)/cm^{-1} 3313 (OH), 2911 (CH), 1257 (ArO), 904 (SiOAr), 727 ($Si(C_2H_3)_3$); δ_H (400 MHz; $CDCl_3$) 7.23 (d, *J* 8.70 Hz, 2H), 6.86 (d, *J* 8.5 Hz, 2H), 4.59 (d, *J* 5.0 Hz, 2H), 0.94 (t, *J* 7.9 Hz, 9H), 0.69 (q, *J* 7.9 Hz, 6H); δ_C (100 MHz; $CDCl_3$) 156.8, 135.0, 129.9, 121.2, 65.8, 6.7, 5.0; MS *m/z* (APCI) 221.1 (100%, $[M–OH]^+$); HRMS *m/z* (APCI) Calcd. for $C_{13}H_{21}OSi$ $[M–OH]^+$: 221.1356, found: 221.1356.

2.7.10 Triethyl(4-(2-((triethylsilyl)oxy)ethyl)phenoxy)silane, 24 (3)

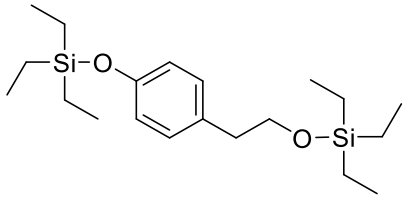

To a solution of 4-hydroxyphenethyl alcohol (500 mg, 3.6 mmol) in anhydrous DMF (20 mL) was added chlorotriethylsilane (1.2 mL, 7.2 mmol) and Et_3N (1 mL, 7.2 mmol). The mixture was stirred for 16 h, after which hexane (200 mL) was added and the mixture washed with H_2O (200 mL). The organic phase was then dried ($MgSO_4$) and concentrated under reduced pressure. The residue was purified by silica gel chromatography using the eluent noted below to yield **24** as a colorless oil (540 mg, 40%); R_f 0.74 (hexane:EtOAc 2:1); ν_{max} (oil)/cm^{-1} 2910 (CH), 1508 (C-C), 1257 (ArO), 1091 ($SiOC_2H_4$), 907 (SiOAr), 727 ($Si(C_2H_3)_3$); δ_H (400 MHz; $CDCl_3$) 7.04 (d, , *J* 8.6 Hz, 2H), 6.77 (d, *J* 8.5 Hz, 2H), 3.73 (t, *J* 7.2 Hz, 2H), 2.72 (t, *J* 7.2 Hz, 2H), 0.93 (t, *J* 7.9 Hz, 9H), 0.86 (t, *J* 7.9 Hz, 9H), 0.67 (q, *J* 7.9 Hz, 6H), 0.50 (q, *J* 7.8 Hz, 6H); δ_C (100 MHz; $CDCl_3$) 154.6, 132.2, 130.6, 120.3, 64.6, 39.0, 6.8, 6.7, 5.0, 4.3; MS *m/z* (APCI) 235 (100%, $[M-C_6H_{15}OSi]^–$); HRMS *m/z* (APCI) Calcd. for $C_{13}H_{21}OSi$ $[M–C_6H_{15}OSi]^–$: 235.1518, found: 235.1510.

2.7.11 4-(2-((Triethylsilyl)oxy)ethyl)phenol, 25

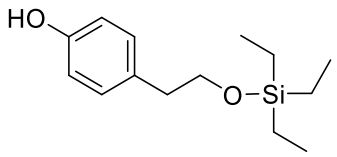

Compound **25** was isolated as a pale yellow oil from the same reaction mixture as **24** during column chromatography as a dark yellow oil (210 mg, 23%); R_f 0.47 (hexane:EtOAc 2:1); ν_{max} (oil)/cm^{-1} 3291 (OH), 2910 (CH), 1235 (ArO), 1084 ($SiOC_2H_4$), 743 ($Si(C_2H_3)_3$); δ_H (400 MHz; $CDCl_3$) 7.06 (d, *J* 8.5 Hz, 2H), 6.77 (d, *J* 8.5 Hz, 2H), 3.75 (t, *J* 7.4 Hz, 2H), 2.74 (t, *J* 7.4 Hz, 2H), 0.87 (t, *J* 7.9 Hz, 9H), 0.53 (q, *J* 7.9 Hz, 6H); δ_C (100 MHz; $CDCl_3$) 154.9, 131.3, 130.8, 115.7, 64.9, 38.8, 6.8, 4.4; MS *m/z* (ES^+) 275 (100%, $[M+Na]^+$); HRMS *m/z* (ES^+) Calcd. for $C_{14}H_{24}O_2SiNa$ $[M+Na]^+$: 275.1438, found: 275.1434.

2.7.12 2-(4-(Triethylsilyl)oxy)phenyl)ethanol, 26 (3)

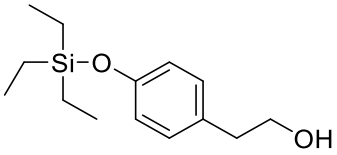

Compound **26** was isolated as a pale yellow oil from the same reaction mixture as **24** during column chromatography as a pale yellow oil (127 mg, 14%); R_f 0.27 (hexane:EtOAc 2:1); ν_{max} (oil)/cm^{-1} 3317 (OH), 2911 (CH), 1257 (ArO), 907 (SiOAr), 730 ($Si(C_2H_3)_3$); δ_H (400 MHz; $CDCl_3$) 7.07 (d, *J* 8.6 Hz, 2H), 6.81 (d, *J* 8.5 Hz, 2H), 3.84-3.85 (m, 2H), 2.76 (t, *J* 6.5 Hz, 2H), 0.94 (t, *J* 7.9 Hz, 9H), 0.68 (q, *J* 7.9 Hz, 6H); δ_C (100 MHz; $CDCl_3$) 155.5, 132.0, 131.1, 121.1, 64.4, 38.7, 6.7, 5.0; MS *m/z* (ES^+) 275.1419 (100%, ($[M+Na]^+$); HRMS *m/z* (APCI) Calcd. for $C_{14}H_{23}OSi$ $[M-OH]^+$: 235.1513, found: 235.1503.

2.7.13 Triethyl(3-(4-((triethylsilyl)oxy)phenyl)propoxy)silane, 27

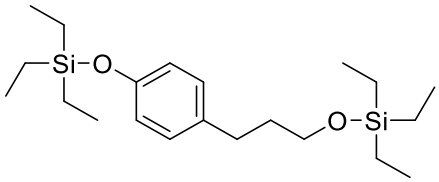

To a solution of 4-(3-hydroxypropyl)phenol (500 mg, 3.28 mmol) in anhydrous DMF (20 mL) was added chlorotriethylsilane (0.82 mL, 4.9 mmol) and Et_3N (1 mL, 7.2 mmol). The mixture was stirred for 4 h, after which hexane (200 mL) was added and the mixture washed with H_2O (200 mL). The organic phase was then dried ($MgSO_4$) and concentrated under reduced pressure. The residue was separated by silica gel chromatography using the eluent noted below to yield **27** as a colorless oil (494 mg, 40%); R_f 0.72 (hexane:EtOAc 2:1); ν_{max} (oil)/cm^{-1} 2875 (CH),1508 (C-C), 1257 (ArO), 1095 ($SiOC_3H_6$), 908 (SiOAr), 728 ($Si(C_2H_3)_3$); δ_H (400 MHz; $CDCl_3$) 7.03 (d, *J* 8.6 Hz, 2H), 6.78 (d, *J* 8.5 Hz, 2H), 3.59 (t, *J* 6.5 Hz, 2H), 2.57 (t, *J* 7.7 Hz, 2H), 1.76 (dt, *J* 14.9 Hz, *J* 7.1 Hz, 2H), 0.95 (t, *J* 7.0 Hz, 9H), 0.92 (t, *J* 7.0 Hz, 9H), 0.70 (q, *J* 7.9 Hz, 6H), 0.55 (q, *J* 7.8 Hz, 6H); δ_C (100 MHz; $CDCl_3$) 154.2, 135.5, 129.9, 120.3, 62.5, 34.7, 31.4, 6.8, 6.7, 5.0, 4.5; MS *m/z* (APCI) 381 (100%, $[M+H]^+$); HRMS *m/z* (APCI) Calcd. for $C_{19}H_{37}O_2Si_2$ $[M+H]^+$: 381.2640, found: 381.2636.

2.7.14 4-(3-((Triethylsilyl)oxy)propyl)phenol, 28

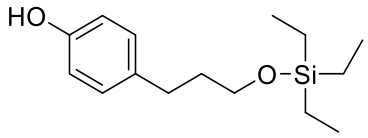

Compound **28** was isolated as a pale yellow oil from the same reaction mixture as **27** during column chromatography as a colorless oil (182 mg, 20%); R_f 0.48 (hexane:EtOAc 2:1); ν_{max} (oil)/cm^{-1} 3310 (OH), 2875 (CH), 1233 (ArO), 1094 ($SiOC_3H_6$), 727 ($Si(C_2H_3)_3$); δ_H (400 MHz; $CDCl_3$) 7.05 (d, *J* 8.5 Hz, 2H), 6.76 (d, *J* 8.5 Hz, 2H), 3.59 (t, *J* 6.4 Hz, 2H), 2.56 (t, *J* 7.7 Hz, 2H), 1.76 (dt, *J* 14.9 Hz, *J* 7.1 Hz, 2H), 0.91 (t, *J* 7.9 Hz, 9H), 0.56 (q, *J* 7.9 Hz, 6H); δ_C (100 MHz; $CDCl_3$) 154.2, 135.0, 130.1, 115.7, 62.5, 34.8, 31.3, 6.8, 4.5; MS *m/z* (ES^+) 267.1 $[M+Na]^+$, (100%), HRMS *m/z* (ES^+) Calcd. for $C_{15}H_{26}NO_3SiNa$ $[M+Na]^+$: 267.1775, found: 267.1762.

2.7.15 3-(4-((Triethylsilyl)-oxy)phenyl) propan-1-ol, 29

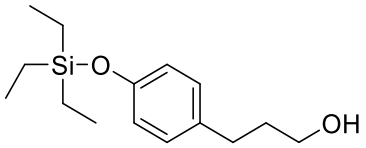

Compound **29** was isolated as a pale yellow oil from the same reaction mixture as **27** during column chromatography as a colorless oil (103 mg, 8%); R_f 0.23 (hexane:EtOAc 2:1); ν_{max} (oil)/cm^{-1} 3304 (OH), 2875 (CH), 1256 (ArO), 907 (SiOAr), 729 ($Si(C_2H_3)_3$); δ_H (400 MHz; $CDCl_3$) 7.04 (d, *J* 8.6 Hz, 2H), 6.78 (d, *J* 8.5 Hz, 2H), 3.63 (t, *J* 6.1 Hz, 2H), 2.60 (t, *J* 7.6 Hz, 2H), 1.82 (dt, *J* 14.7 Hz, *J* 7.0 Hz, 2H), 0.93 (t, *J* 7.9 Hz, 9H), 0.68 (q, *J* 7.7 Hz, 6H); δ_C (100 MHz; $CDCl_3$) 154.3, 134.7, 129.9, 120.4, 62.7, 34.5, 31.4, 6.7, 5.0; MS *m/z* (APCI) 267 (100%, $[M+H]^+$); HRMS *m/z* (APCI) Calcd. for $C_{15}H_{27}NO_3Si$ $[M+H]^+$: 267.1775, found: 267.1774.

2.7.16 4-Nitrophenoxy pivalate, Piv-ONp, 30

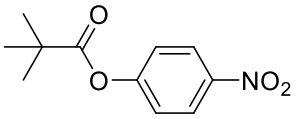

To a solution of 4-nitrophenol (1128 mg, 8.11 mmol) in anhydrous Et_2O (20 mL) was added pivaloyl chloride (1 mL, 8.11 mmol) and pyridine (0.97 mL, 12.16 mmol). The mixture stirred for 30 min, hexane (50 mL) added and the mixture washed with H_2O (50 mL). The organic phase was dried with $MgSO_4$ and concentrated under reduced pressure. The residue was purified by silica gel chromatography using the eluent noted below to the desired product as a white powder (1752 mg, 96%); R_f 0.26 (hexane:EtOAc, 20:1); ν_{max} (solid)/cm^{-1} 1756 (COO), 1590 (C-C), 1346 (NO_2), 1092 (C-O); δ_H (400 MHz; $CDCl_3$) 8.28 (d, *J* 9.2 Hz, 2H), 7.28 (d, *J* 9.2 Hz, 2H), 1.39 (s, 9H); δ_C (100 MHz; $CDCl_3$) 176.0, 155.9, 145.1, 125.1, 122.4, 39.3, 27.0; MS *m/z* (ES^+) 224 (100%, $[M+H]^+$); HRMS *m/z* (ES^+) Calcd. for $C_{11}H_{15}NO_3$ $[M+H]^+$: 224.0917, found: 224.0919.

2.7.17 4-Nitrophenyl pivalamide, Piv-NHNp, 31

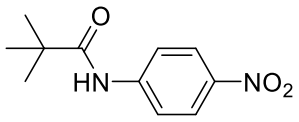

To a solution of 4-nitroaniline (500 mg, 3.6 mmol) in anhydrous Et_2O (20mL) was added pivaloyl chloride (0.66 mL, 5.4 mmol) and pyridine (0.58 mL, 7.2 mmol). The mixture stirred for 30 min, hexane (100 mL) added and the mixture washed with H_2O (100 mL). The organic phase was then dried with $MgSO_4$ and concentrated under reduced pressure. The residue was purified by silica gel chromatography using the eluent noted below to yield **31** as a white powder (122 mg, 10%); R_f 0.57 (hexane:EtOAc, 2:1); ν_{max} (solid)/cm^{-1} 3304 (N-H), 1788 (CONH), 1594 (C-C), 1380 (NO_2); δ_H (400 MHz; $CDCl_3$) 8.23 (d, *J* 9.1 Hz, 2H), 7.76 (d, *J* 9.2 Hz, 2H), 1.36 (s, 9H); δ_C (100 MHz; $CDCl_3$) 144.2, 125.0, 119.1, 102.1, 100.2, 40.0, 27.5; MS *m/z* (ES^+) 223.1 (100%, $[M+H]^+$); HRMS *m/z* (ES^+) Calcd. for $C_{11}H_{15}NO_3$ $[M+H]^+$: 223.1076, found: 223.1082.

2.8 Computational modelling.

2.8.1 Homology modelling

A homology model was built using SWISS-MODEL.(17, 18) Following removal of amino acids comprising the signal peptide and pro-peptide region of the protein, the target sequence Q9GV98_SUBDO (UniProtKB) / CAI46305 (Genbank) was submitted to the SWISS-MODEL template library and searched with BLAST(19) and HHBlits(20) for primary amino acid sequences with regions of similarity. A total of 378 templates were found. Regions of similarity identified were verified by additional EMBOSS Needle Pairwise Sequence Alignment.

This comparative analysis resulted in the following alignment:

```
Sili_SubDo  DYPEAVDWRTKGAVTAVKDQGDCGASYAFSAMGALEGANALAKGNAVSLSEQNIIDCSIPYGN
Human_CathL EAPRSVDWREKGYVTPVKNQGQCGSAWAFSATGALEGQMFRKTGRLISLSEQNLVDCSGPQGN

Sili_SubDo  HGCHGGNMYDAFLYVIANEGVDQDSAYPFVGKQSSCNYNSKYKGTSMSGMVSIKSGSESDLQA
Human_CathL EGCNGGLMDYAFQYVQDNGGLDSEESYPYEATEESCKYNPKYSVANDTGFVDIPK-QEKALMK
```

```
Sili_SubDo  AVSNVGPVSVAIDGANSAFRFYYSGVYDSSRCSSSSLNHAMVVTGYGSY----NGKKYWLAKN
Human_CathL AVATVGPISVAIDAGHESFLFYKEGIYFEPDCSSEDMDHGVLVVGYGFESTESDNNKYWLVKN

Sili_SubDo  SWGTNWGNSGYVMMARNKYNQCGIATDASYPTL
Human_CathL SWGEEWGMGGYVKMAKDRRNHCGIASAASYPTV
```

Sequence Similarity – 0.45

Sequence Identity – 51.15

The target-template alignment of 2NQD (PDB) was used by ProMod Version 3.70 to construct a 3D model of silicatein based on coordinates conserved between the protein of interest and the template sequence/structure. The fragment library remodeled insertions and deletions from sequence alignment, relevant side chains were rebuilt and geometry was regularized using a force field.(11)

2.8.2 Molecular dynamics simulations

The model set-up followed methods as previously described.(21) Hydrogen atoms were added to the model with pdb2pqr server at pH 7 using PropKa.(22) Titratable amino acid residues were subsequently manually checked for the correct protonation states and all three histidine residues (His_{64}, His_{67} and His_{165}) were taken as singly protonated: His_{64} and His_{67} at Nδ and His_{165} at the Nε. All Glu and Asp side chains were deprotonated and all Arg and Lys side chains were protonated, which gave the protein an overall charge of –2. Topology data, together with electrostatic and bonding parameters for the substrates were created with Swissparam.(23) In an initial step, the hydrogen atoms were energy minimized, while the backbone was kept fixed. Subsequently, the substrate was inserted into the structure and the enzyme-substrate model was subjected to an energy minimization procedure with the CHARMM program.(24) Thereafter, the protein was embedded in a water sphere with a radius of 40 Å and followed by a 100 ps equilibration using the Langevin dynamics. The solvation and equilibration were done repeatedly until the system became saturated. After 17 iterations, a total 4,737 TIP3 water molecules were added to the system. Finally, the protein was neutralized with 14 Cl^- and 8 Mg^{+2} ions. Prior to the MD simulation, the system was energy minimized without constraints, heated to 300K, and then equilibrated. Two separate MD simulations were conducted, each for time period of 1 ns. In the first simulation the substrate was constrained by fixing its nuclear

coordinates, while in the second one the protein and the substrates were allowed to move freely during MD.

3 References for Supporting Information

1. Hellal M, Falk FC, Wolf E, Dryzhakov M, & Moran J (2014) Breaking the dichotomy of reactivity vs. chemoselectivity in catalytic S_N1 reactions of alcohols. *Org. Biomol. Chem.* 12(31):5990-5994.
2. Fernandes RA, Gholap SP, & Mulay SV (2014) A facile chemoselective deprotection of aryl silyl ethers using sodium hydride/DMF and in situ protection of phenol with various groups. *RSC Adv.* 4(32):16438-16443.
3. Yeom C-E, Kim YJ, Lee SY, Shin YJ, & Kim BM (2005) Efficient chemoselective deprotection of silyl ethers using catalytic 1-chloroethyl chloroformate in methanol. *Tetrahedron* 61(52):12227-12237.
4. Schraml J, Chvalovský V, Jancke H, & Engelhardt G (1977) Steric effects in ^{29}Si and ^{13}C N.m.r. spectra of trimethylsiloxy-substituted benzenes. *Org. Magn. Reson.* 9(4):237-238.
5. Rakita PE, Worsham LS, & Srebro JP (1976) ^{13}C n.m.r. studies of organosilanes: II - substituent chemical shift parameters for alkoxysilanes. *Org. Magn. Reson.* 8(6):310-316.
6. Blechta V, *et al.* (2012) The effect of solvent accessible surface on Hammett-type dependencies of infinite dilution ^{29}Si and ^{13}C NMR shifts in ring substituted silylated phenols dissolved in chloroform and acetone. *Magn. Reson. Chem.* 50(2):128-134.
7. Socrates G (2001) Infrared and Raman Characteristic Group Frequencies: Tables and Charts. (Wiley, Chichester), 3rd Ed, pp 241-246.
8. Schröder HC, *et al.* (2012) Acquisition of structure-guiding and structure-forming properties during maturation from the pro-silicatein to the silicatein form. *J. Biol. Chem.* 287(26):22196-22205.
9. Ho SN, Hunt HD, Horton RM, Pullen JK, & Pease LR (1989) Site-directed mutagenesis by overlap extension using the polymerase chain-reaction. *Gene* 77(1):51-59.
10. Poschner BC, Reed J, Langosch D, & Hofmann MW (2007) An automated application for deconvolution of circular dichroism spectra of small peptides. *Anal. Biochem.* 363(2):306-308.

11. Guex N & Peitsch MC (1997) SWISS-MODEL and the Swiss-Pdb Viewer: An environment for comparative protein modeling. *Electrophoresis* 18(15):2714-2723.
12. Adamson DH, Dabbs DM, Morse DE, & Aksay IA (2004) Non-peptide, silicatein α inspired silica condensation catalyst. *Polym. Mater.: Sci. Eng.* 90:239-240.
13. Coradin T, Eglin D, & Livage J (2004) The silicomolybdic acid spectrophotometric method and its application to silicate/biopolymer interaction studies. *Spectroscopy* 18(4):567-576.
14. Iler RK (1979) *The Chemistry of Silica: Solubility, Polymerization, Colloid and Surface Properties, and Biochemistry*, (Wiley, New York), pp 95-100.
15. Tong X, Tang T, Feng ZL, & Huang BT (2002) Preparation of polymer/silica nanoscale hybrids through sol-gel method involving emulsion polymers. II. Poly(ethyl acrylate)/SiO2. *J. Appl. Polym. Sci.* 86(14):3532-3536.
16. Muller WEG, *et al.* (2011) Hardening of bio-silica in sponge spicules involves an aging process after its enzymatic polycondensation: Evidence for an aquaporin-mediated water absorption. *Biochim. Biophys. Acta, Gen. Subj.* 1810(7):713-726.
17. Biasini M, *et al.* (2014) SWISS-MODEL: modelling protein tertiary and quaternary structure using evolutionary information. *Nucleic Acids Res.* 42(W1):W252-W258.
18. Arnold K, Bordoli L, Kopp J, & Schwede T (2006) The SWISS-MODEL workspace: a web-based environment for protein structure homology modelling. *Bioinformatics* 22(2):195-201.
19. Altschul SF, *et al.* (1997) Gapped BLAST and PSI-BLAST: a new generation of protein database search programs. *Nucleic Acids Res.* 25(17):3389-3402.
20. Remmert M, Biegert A, Hauser A, & Soding J (2012) HHblits: lightning-fast iterative protein sequence searching by HMM-HMM alignment. *Nat. Methods* 9(2):173-175.
21. Quesne MG, Borowski T, & de Visser SP (2016) Quantum Mechanics/Molecular mechanics modeling of enzymatic processes: caveats and breakthroughs. *Chem. Eur. J.* 22(8):2562-2581.
22. Dolinsky TJ, *et al.* (2007) PDB2PQR: expanding and upgrading automated preparation of biomolecular structures for molecular simulations. *Nucleic Acids Res.* 35(suppl 2):W522-W525.
23. Zoete V, Cuendet MA, Grosdidier A, & Michielin O (2011) SwissParam: A fast force field generation tool for small organic molecules. *J. Comput. Chem.* 32(11):2359-2368.

24. Brooks BR, *et al.* (2009) CHARMM: The biomolecular simulation program. *J. Comput. Chem.* 30(10):1545-1614.